Copy 226
RM L51F14

NACA

RESEARCH MEMORANDUM

COMPARISON OF TRANSONIC CHARACTERISTICS OF LIFTING WINGS

FROM EXPERIMENTS IN A SMALL SLOTTED TUNNEL AND THE

LANGLEY HIGH-SPEED 7- BY 10-FOOT TUNNEL

By William C. Sleeman, Jr., Paul L. Klevatt,
and Edward L. Linsley

Langley Aeronautical Laboratory
Langley Field, Va.

NATIONAL ADVISORY COMMITTEE
FOR AERONAUTICS

WASHINGTON
November 5, 1951

CONFIDENTIAL
SECURITY INFORMATION
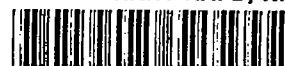
NATIONAL ADVISORY COMMITTEE FOR AERONAUTICS

RESEARCH MEMORANDUM

COMPARISON OF TRANSONIC CHARACTERISTICS OF LIFTING WINGS

FROM EXPERIMENTS IN A SMALL SLOTTED TUNNEL AND THE

LANGLEY HIGH-SPEED 7- BY 10-FOOT TUNNEL

By William C. Sleeman, Jr., Paul L. Klevatt,
and Edward L. Linsley

SUMMARY

A comparison is made of the transonic aerodynamic characteristics
of unswept and 45° sweptback wings tested in the Langley high-speed
7- by 10-foot tunnel and in a 4.5- by 6.25-inch slotted tunnel developed
by the Langley Internal Aerodynamics Section. Two geometrically similar
wings having areas equal to 32 percent and 12 percent of the tunnel cross-
sectional area were tested for both sweep angles to investigate effects
of relative model size in the slotted tunnel. Two slot areas, 1/5 and 1/8
of the horizontal boundaries open, were used in the tests.

It was found that tunnel choking was eliminated and blockage effects
for the wings tested were alleviated by the slotted test section through-
out the Mach number range and lift range investigated. The over-all
transonic aerodynamic characteristics of the four wings tested in the
$\frac{1}{8}$ -open slotted tunnel, neglecting all tunnel boundary corrections, were
consistent with 7- by 10-foot tunnel results throughout the Mach number
range investigated. The amount of slot open area showed a substantial
effect at subsonic Mach numbers on lift-curve slopes, while effects of
relative size of the model predominated at supersonic Mach numbers. Jet-
boundary interference effects in the slotted tunnel, as indicated by
subsonic lift-curve slopes and pitching-moment characteristics near a
Mach number of unity, increased appreciably with model size for the
sweptback wings.

CONFIDENTIAL

INTRODUCTION

The purpose of this investigation was to explore the possibilities and limitations associated with transonic testing of relatively large lifting wings in a rectangular slotted tunnel. The problem of determining subsonic jet-boundary-induced-angle corrections was anticipated in view of the theoretical corrections presented in reference 1 for a circular tunnel. Reference 1 shows that the ratio of closed to total periphery for zero blocking, determined in reference 2 for a circular tunnel, is subject to an appreciable induced-angle correction factor. Consequently, some induced-angle correction might be expected in a rectangular slotted test section designed to eliminate blockage effects. Theoretical induced-angle corrections for rectangular tunnels having partially open horizontal boundaries are not currently available. Difficulties would be expected in evaluating these corrections for lifting wings in subsonic tunnels having multiple-slot or porous walls, and at transonic speeds the problem is further complicated by mixed-flow phenomena.

The present investigation was undertaken as a joint project of the Langley High-Speed 7- by 10-Foot Tunnel Section and the Langley Internal Aerodynamics Section to determine by experiment the magnitude and direction of any differences between the aerodynamic characteristics of several lifting wings tested in the 7- by 10-foot tunnel and those obtained in a tunnel with slotted walls. Aerodynamic characteristics in pitch were obtained for two unswept and two 45° sweptback wings over a Mach number range from 0.70 to 1.30 in a 4.5- by 6.25-inch slotted tunnel developed by the Langley Internal Aerodynamics Section. Two slot-open-area ratios, 1/8 and 1/5 of the horizontal boundaries open (1/13.8 and 1/8.6 of total periphery open), were investigated and effects of model size were studied. Results also were obtained for the large unswept wing tested in the 4.5- by 6.25-inch tunnel with the horizontal boundaries closed and completely open for a comparison of results obtained with the slotted configuration. All data are compared with results for the same wings tested on a reflection plane in the Langley high-speed 7- by 10-foot tunnel for Mach numbers from 0.70 to 1.08. The reflection plane was located outside of the boundary layer on the tunnel side wall. These reflection-plane results were selected to represent data which are regarded as being essentially free from tunnel boundary effects, inasmuch as the model was very small (4.24-inch span) compared to the tunnel size, and the model was believed to be unaffected by the main tunnel boundary layer.

Data obtained on the reflection plane in the Langley high-speed 7- by 10-foot tunnel may not entirely represent free-air results, but these data represent the best available basis for a comparison of the

particular wings used in this investigation. Differences in results from the slotted-tunnel and reflection-plane tests were, in many cases, smaller than those indicated for the same wing plan forms investigated in several different test facilities (reference 3). In the present comparison, relatively small boundary interference effects in the slotted tunnel could be masked by differences in turbulence and Mach number gradients in the two test facilities. The comparison of over-all results, however, provides an indication of first-order tunnel interference effects associated with transonic tests in the slotted tunnel used in this investigation.

Results obtained from the reflection-plane tests in the Langley high-speed 7- by 10-foot tunnel are referred to as 7 by 10 results in the remainder of this paper.

SYMBOLS

C_L lift coefficient (Twice semispan lift/qS)

C_D drag coefficient (Twice semispan drag/qS)

ΔC_D drag coefficient due to lift $\left(C_D - C_{D_{L=0}}\right)$

$C_{D_{L=0}}$ drag coefficient at zero lift

C_m pitching-moment coefficient referred to $0.25\bar{c}$ (Twice semispan pitching moment/$qS\bar{c}$)

C_B bending-moment coefficient due to lift, about root-chord line (at plane of symmetry) $\left(\text{Root bending moment}/q\,\frac{S}{2}\,\frac{b}{2}\right)$

q effective dynamic pressure over span of model, pounds per square foot $\left(\frac{1}{2}\rho V^2\right)$

S twice wing area of semispan model, square feet

$\bar{c}$ mean aerodynamic chord of wing, feet; based on relationship $\frac{2}{S}\int_0^{b/2} c^2 dy$ (using theoretical tip)

c local wing chord, feet

b   twice span of semispan model

ρ air density, slugs per cubic foot

V   free-stream velocity, feet per second

M   effective local Mach number over span of model

y_{cp} lateral center of pressure, percent semispan $\left(100\ C_B/C_L\right)$

α geometric angle of attack, degrees

MODELS AND APPARATUS

Models.- The steel wings used in this investigation were all of
aspect ratio 4 and taper ratio 0.6 and had NACA 65A006 airfoil sections
parallel to the free stream. Two wings having 4.24-inch semispans with
their $\bar{c}/4$ lines unswept and sweptback 45° and two additional wings,
geometrically similar to the first pair but having 2.55-inch semispans,
were tested to study the effect of model size. The areas of these wings
were approximately 32 percent and 12 percent of the slotted-tunnel cross-
sectional area. A drawing of the four wings is presented in figure 1
and the general arrangement of the experimental setup showing the large
unswept wing mounted in the slotted tunnel is shown in figure 2.

The models were mounted through the tunnel wall and attached to an
electrical strain-gage balance which was sealed except for a 0.025-inch
gap around the model root. An end plate was attached to the model for
all tests in the 4.5- by 6.25-inch tunnel (fig. 2(b)) to minimize the
effects of any flow through the gap. A similar arrangement was used
for the 7- by 10-foot tunnel side-wall tests on the small wings while
somewhat larger end plates were used on the large wings (fig. 1). Tests
on several models with the end plate removed and the gap sealed with a
sponge-wiper seal have indicated that the large end plates had a negli-
gible effect except for a small and constant increment in drag coeffi-
cient. Minimum-drag results for the large wings in the 7- by 10-foot
tunnel were obtained with a sponge-wiper seal, and these results are
compared with data obtained in the slotted tunnel with the small end
plates on the wings. Tests on the large unswept wing indicated that
the small end plate used for tests in the slotted tunnel had essentially
no effect on the minimum drag.

Apparatus.- Test facilities of the Langley Internal Aerodynamics
Section were utilized for all tests conducted in the 4.5- by 6.25-inch
tunnel. A photograph of the tunnel installed in the pressure chamber

with one side plate removed is presented as figure 3. The 4.5- by 6.25-inch rectangular cross section of the channel was constant throughout the 15.0-inch-long slotted region. The tunnel contraction ratio was approximately 25 to 1. The slotted boundaries were obtained by spacing 0.25- by 0.50-inch bars across the tunnel (fig. 2(b)) 0.037 inch apart, giving a ratio of open area to floor and ceiling area of 1/8. An open-area ratio of 1/5 was obtained by spacing the bars 0.066 inch apart. For the tests with open horizontal boundaries, the bars were removed and the entrance nozzle extended 5 inches downstream, terminating in a sharp-edge lip 2 inches ahead of the wing reference axis. A rounded collector was installed 7.25 inches downstream of the wing reference axis. For the closed-tunnel tests the slotted boundaries were replaced by a solid floor and ceiling.

Static-pressure surveys in the empty tunnel were made with a $\frac{1}{16}$ - inch-diameter tube having four static orifices of 0.014-inch diameter. The longitudinal surveys along the center of the empty tunnel indicated that the Mach number gradient in the portion of the tunnel occupied by the model was less than 0.01 above or below the average Mach number throughout the Mach number range for the $\frac{1}{8}$ - open tunnel. The gradients were also of this magnitude up to M = 1.10 for the $\frac{1}{5}$ - open-tunnel configuration. The Mach number variation over the model with the $\frac{1}{5}$ - open floor and ceiling increased to about ±0.03 at M = 1.15 and data were not obtained above M = 1.15. A lateral survey indicated that the Mach number was essentially constant across the tunnel in the region of the model. The extent of the boundary layer (M < 95 percent free-stream Mach number) was about 0.01 inch.

The results which were used to represent free-air conditions were obtained by using the Langley high-speed 7- by 10-foot tunnel side-wall reflection plane described in reference 3. The Mach number gradients on the side-wall reflection plane were less than ±0.01 up to M = 0.95 and increased to about ±0.02 at M = 1.08. The reflection-plane boundary layer was about 0.01 inch at the model.

Schlieren pictures were obtained with a parallel-beam, two-pass system utilizing one parabolic mirror and a plane front-surface mirror mounted in the tunnel wall as a reflecting mirror. The light source was a high intensity spark of approximately 4 microseconds duration. For all observations the knife edge was normal to the flow. The small unswept wing was mounted through the plane mirror, the clearance between the wing surface and cutout being approximately 0.05 inch, except at the leading and trailing edges where the clearance was approximately 0.10 inch. The

wing end plate was replaced by a sponge-wiper seal bearing on the rear mirror surface for these tests.

TESTS AND RESULTS

Test conditions.- Subsonic tests below $M = 0.95$ were run with air supplied at atmospheric total pressure; for the remainder of the tests, total pressures above atmospheric were used. For both stagnation conditions, subatmospheric static pressure was maintained in the chamber surrounding the test section by an external pump. Air flow through the slots was effected by the reduced pressure in the chamber and the air was removed from the chamber through the circular opening shown in figure 3 on the downstream end of the tunnel assembly. Minimum-drag results were obtained from tests through the Mach number range at elevated stagnation pressures at zero wing lift. Figure 4 shows the variation of Reynolds number based on the wing mean aerodynamic chord with Mach number for the two stagnation conditions. Reynolds number differences associated with the two stagnation conditions had no appreciable effect on the over-all results obtained in the slotted tunnel from $M = 0.95$ to $M = 1.00$. Reynolds numbers based on free-stream velocity (neglecting stream turbulence) in the 7- by 10-foot tunnel were the same as those indicated for the atmospheric stagnation condition in the slotted tunnel.

Test procedure.- Data were obtained through the angle-of-attack range at each Mach number. The angle-of-attack range was $-5°$ to $20°$ for most of the tests of the small wings and $-5°$ to $12°$ or to limiting angle for the large wings. The angle of attack of the large wings was limited at the higher Mach numbers by the forces exerted on the strain-gage balance.

The Mach number over the model was determined from the empty-tunnel surveys for each floor and ceiling configuration. In the empty-tunnel surveys the test-section Mach number was calibrated against static pressure in the chamber surrounding the test section. The Mach numbers selected for the tests were accordingly set by the reference chamber pressure and free-stream total pressure.

Corrections.- No induced-angle or blockage corrections have been applied to the data.

Results.- The basic data of this investigation are presented in figures 5 to 9 and the over-all results are presented in summary plots (figs. 10 to 16). The discussion of over-all effects will, in general, be based on these summary figures. In some cases, especially where nonlinear variations of C_m and C_L with α exist, the significance

of the slope parameters is somewhat decreased. For this reason, all the
basic data from which the summary plots were obtained are presented. In
most instances, the slopes were averaged over an angle-of-attack range of
$\pm 4^\circ$ or up to an angle at which obvious departures from linearity occurred.
In some of the data for the small wings in the slotted tunnel, the effects
of laminar separation were evident near zero lift and in these instances
the pitching-moment slopes were determined over a lift-coefficient range
of $C_L = 0.05$ to 0.30 where these laminar-separation effects were
probably minimized.

Since the high-speed 7- by 10-foot tunnel side-wall results were
obtained only up to $M = 1.08$, some data from the transonic bump of the
high-speed 7- by 10-foot tunnel are presented for comparison with the
slotted-tunnel results for the large wings at $M = 1.20$. The 7 by
10 side-wall data for the large wings presented herein and bump data at
lower Mach numbers are presented in reference 3, which includes an
analysis of differences found in these data. The small wings used in
this investigation were tested in the Langley 6-inch supersonic tunnel
at $M = 1.38$ (reference 4) and some of the results are included for
comparison at the highest Mach numbers attained in the slotted tunnel.

DISCUSSION

Limited results for the large unswept wing tested in the 4.5- by
6.25-inch tunnel with the horizontal boundaries open and closed are
presented in figure 5. Jet-boundary-induced angles and blockage correc-
tions have not been applied to these data in order to illustrate the
magnitude of discrepancies compared to free-air results that would be
expected in testing a model of this relative size with corrections
neglected. Large differences in lift and drag characteristics are
evident and indicate the change in sign of angularity induced by
the jet boundaries as the solid horizontal boundaries are removed. In
general, the pitching-moment results for the open and closed configurations
are consistent with effects that can be attributed to differences in
streamline curvature. Uncorrected data for the same wing tested in the

tunnel with the $\frac{1}{8}$- open slotted floor and ceiling (fig. 6) showed very

good agreement with 7 by 10 results, the agreement indicating that tunnel
choking was essentially eliminated and that jet-boundary-induced effects
were small for this tunnel configuration. An analysis of the results of
all the wings tested in the slotted tunnel is given in the following
sections.

Lift

Unswept wings.- The results for the $\frac{1}{8}$- open configuration are in
very good agreement with the 7 by 10 data for both the large and small
unswept wings, the slotted-tunnel results being slightly lower up to a
Mach number of unity (fig. 10). At supersonic Mach numbers the lift-
curve slopes for the large wing obtained in the slotted tunnel appeared
to be somewhat higher than would be expected from the 7 by 10 side-wall
data and bump data at $M = 1.18$. Lift-curve slopes for the small wing
in the slotted tunnel were in excellent agreement with 7 by 10 data at
low-supersonic speeds where a comparison could be made. At higher speeds
an extrapolation of the slotted-tunnel data to $M = 1.38$ would agree
well with the 6-inch supersonic tunnel point shown (obtained from
reference 4).

The results in the slotted tunnel for both the large and small wings
agree well with the 7 by 10 data on the large wing with regard to over-
all trends with Mach number. While some differences are evident in the
over-all shape of the lift-slope variation with Mach number between the
7 by 10 results for the large and small wings, the slope values at a
given Mach number are in fairly good agreement. Consideration of lift
slopes through zero angle of attack and lift characteristics at high
angles (fig. 7(a)) indicates that the results for the small unswept wing
in the $\frac{1}{8}$- open slotted tunnel were fairly close to the characteristics
that would be expected in free air throughout the Mach number range
investigated.

45° sweep.- Lift-curve slopes for the large sweptback wing in the
slotted tunnel were appreciably lower than those obtained from the 7 by
10 side-wall tests (fig. 10), whereas results for the small swept wing
compared more favorably in the two test facilities. The lift slopes for
the small wing in the slotted tunnel were in fairly good agreement with
7 by 10 results throughout the Mach number range, the $\frac{1}{8}$- open results
closely approaching the 6-inch tunnel point at $M = 1.38$.

The test points for both swept wings show some nonlinearities in
the lift curves and attention should be called to the basic data
(figs. 8(a) and 9(a)). Although differences in lift slopes of the large
swept wing are evident for the 7 by 10 and slotted-tunnel data through
zero lift, it was observed that the over-all shape of the curves at
higher lift coefficients were similar (fig. 8(a)). It would thus appear
that differences in lift results for the large swept wing at subsonic
speeds were mainly associated with jet-boundary-induced-angle corrections.
The magnitude of the lift slopes for the large swept wing in the slotted
tunnel appears to indicate some effect of sweepback on the subsonic

induced-angle corrections for a swept wing of this relative size. The
basic data for the small swept wing in the slotted tunnel (fig. 9(a))
show some nonlinearities in the test points for lift near zero angle of
attack. This nonlinear variation is probably due to laminar-separation
effects associated with low Reynolds numbers found on this wing also in
tests in the 6-inch tunnel (reference 4). While some differences in lift
slope are shown in figure 10, the basic data of figure 9(a) show very
good over-all agreement in lift especially at positive angles of attack
up to about the maximum angle obtained.

Effect of model size and slot area.- Some interesting observations
may be made regarding the effects of open-area ratio and model size in
the slotted tunnel from the results of the unswept wings (fig. 11). At

subsonic Mach numbers, results obtained in the $\frac{1}{8}$ - open slotted tunnel

for the large and small wings were in agreement and the effects of
increasing the slot area to 1/5 open were more pronounced for the large
wing than for the small wing. Above M = 1.00, open-area effects were
very small and the lift slopes were influenced primarily by model size
in the slotted tunnel.

The swept wings (fig. 11) showed roughly the same slot-area effects
as the unswept wings; however, the lift results of the swept wings were
influenced mainly by model size throughout most of the Mach number range
investigated.

In general, jet-boundary interference effects were dependent on slot
area at subsonic speeds and model size at supersonic speeds, these inter-
ference effects being relatively insensitive to slot area above M ≐ 1.00.
Some reduction in slot area below 1/8 open would be necessary to afford
results free of induced-angle corrections at subsonic speeds for the
four wings tested.

Pitching Moments

Unswept wings.- A summary of the pitching-moment characteristics at
low lift is presented in figure 12. While some slope differences between
the slotted-tunnel and 7 by 10 results are apparent for both the large
and small unswept wings, the basic data afford a somewhat more significant
comparison of over-all pitching-moment characteristics due to the limited
lift range for the slopes of figure 12. It should be pointed out with
reference to the pitching-moment slopes that the differences shown for
both the unswept and swept wings are generally of the same order as those
shown for these wing plan forms from the comparison of sting data obtained
in the Langley 8-foot high-speed tunnel and the Langley high-speed 7- by
10-foot tunnel (reference 3). These differences between the slotted-
tunnel and 7 by 10 results therefore should not necessarily be inter-
preted as indicating blockage effects in the slotted tunnel.

In general, the pitching-moment curves for the large wing (fig. 6(b)) obtained in the slotted tunnel are in good agreement with the 7 by 10 side-wall data throughout the Mach number range and with the bump data at M = 1.18, particularly as regards the lift coefficient at which inflections and rapid changes in the pitching-moment curves occur.

Differences in the basic pitching-moment data for the small wing (fig. 7(b)) are evident below M = 1.00. The pitching-moment behavior near zero lift in the slotted tunnel appeared to show effects associated with low Reynolds numbers while the 7 by 10 side-wall results did not show this behavior. Pitching moments obtained in the slotted tunnel were negative at zero lift; this result suggests the possibility of a difference in transition points on the upper and lower surfaces of the wing at a critical low Reynolds number. An explanation of the pitching-moment comparison is believed to be in the different turbulence levels of the 7- by 10-foot tunnel and the slotted tunnel. The flow in the slotted tunnel was very steady because of the large contraction ratio and screens placed upstream of the test section, whereas the flow for the 7 by 10 wall setup was unsteady by comparison. It is believed, therefore, the Reynolds number effects on both the small swept and unswept wings were masked by turbulent flow conditions in the 7- by 10-foot tunnel, which probably increased the effective test Reynolds numbers. At Mach numbers of unity and above, the pitching-moment curves are in very good agreement in the positive lift-coefficient range. The unsymmetrical variation of pitching moment again may possibly be due to unsymmetric separation associated with low Reynolds number.

45° sweep.- The pitching-moment characteristics at low lift for the swept wings are presented in figure 12. The over-all variation of pitching-moment slope with Mach number for both wings is consistent with the 7 by 10 results and trends for the small wing in the $\frac{1}{8}$-open tunnel agree

very well with the slope value obtained in the 6-inch tunnel at M = 1.38 (reference 4). Again, reference to the basic data for these wings should be made for a complete comparison of results.

Figure 8(b) shows excellent agreement for the large wing throughout the lift-coefficient range up to about M = 0.93. Above this Mach number the data compared favorably over only a small lift range around zero lift. Pitching-moment curves obtained in the slotted tunnel show a fairly abrupt deviation from 7 by 10 results at Mach numbers between M = 0.95 and M = 1.08 at about 0.2 lift coefficient. Above M = 1.10 the break is delayed somewhat and at M = 1.20 the data are in good agreement with the bump data up to about C_L = 0.30. The early departure of these large-wing data from 7 by 10 results at Mach numbers near M = 1.0 is unexplained, and in the supersonic region the departures may be due to

reflected-shock phenomena. The pitching-moment curves for the large swept wing were in excellent agreement with those of the small swept wing at the two highest Mach numbers; therefore, it appears that reflections probably did not strike the large wing up to $C_L = 0.30$.

The Reynolds number range for the small swept wing was the same as for the small unswept wing which was subject to effects of low Reynolds numbers in the slotted tunnel. Nonlinearities in the pitching-moment curves of the small swept wing occur at low lift coefficients in the slotted tunnel up to about $M = 0.95$ and consequently pitching-moment slopes have decreased significance in this Mach number range and are not presented in the summary plot (fig. 12). At Mach numbers above $M = 0.95$ the over-all pitching-moment characteristics were in very good agreement, especially as regards variations with lift at high angles of attack.

<center>Drag</center>

Drag at zero lift.- A summary of the minimum-drag characteristics for all of the wings tested is presented in figure 13. Included in the results for the large wings are some drag data (reference 3) obtained from a rocket-model investigation conducted by the Langley Pilotless Aircraft Research Division. These rocket data were obtained with the wings on a fuselage having a cylindrical section at the wing root. The drag of the fuselage alone has been subtracted from the complete-model drag and the values presented represent wing plus interference drag.

Results for the large unswept wing in the slotted tunnel are in excellent agreement in magnitude and rate of drag rise with both the 7 by 10 results and rocket data. The good over-all agreement of these data indicates that tunnel choking was eliminated and blockage effects were alleviated by the slotted test sections used.

Data for the large swept wing in the slotted tunnel agree well with 7 by 10 results in regard to magnitude, but the drag rise is delayed somewhat in the slotted tunnel. These drag differences suggest the possibility that the results for this wing may have been affected by the presence of the tunnel boundaries near sonic speeds. A comparison with rocket data near $M = 1.0$ is more favorable; however, definite conclusions regarding adverse tunnel effects on the large swept wing cannot be made on the basis of the fairly small differences shown.

The small drag forces and flow unsteadiness in the 7- by 10-foot tunnel caused an appreciable reduction in accuracy of the strain-gage balance in measuring minimum drag coefficients for the small wings; consequently, these results are not presented. In general, the results for the small wings in the slotted tunnel obtained at elevated stagnation

pressures compare favorably with the large wings and with the results from the 6-inch supersonic tunnel at M = 1.38.

Drag due to lift.- A limited comparison of drag due to lift through the Mach number range is presented in figures 14 and 15. The basic data (figs. 6(c), 7(c), 8(c), and 9(c)) show good agreement for slotted-tunnel and 7 by 10 results in the low-lift-coefficient range. At moderate and high lift coefficients differences in drag were evident in many cases. The magnitude of the drag at a given lift coefficient (figs. 14 and 15) indicated that the resultant force vector was inclined at an angle approximately normal to the wing chord, in which case the drag due to lift should be approximately equal to $C_L \tan \alpha$. Values of $C_L \tan \alpha$ are presented in figures 14 and 15 for a comparison with the drag. The agreement of this parameter with the drag coefficient is very good as regards trends with Mach number and magnitude of discrepancies between 7 by 10 and slotted-tunnel results. It appears from this comparison that differences in drag due to lift in the two test facilities may therefore be accounted for by differences in angle of attack required to support a given lift rather than a result of tunnel blockage effects.

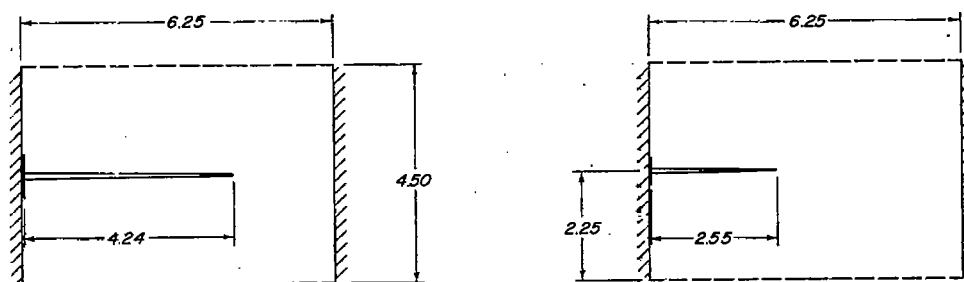An over-all evaluation of the drag results indicates that tunnel choking was eliminated and blockage effects were alleviated by the slotted test section throughout the lift range investigated for the wings tested.

Bending Moments

A summary of the bending-moment characteristics of the large wings is presented in figure 16. No attempt has been made to determine effects of the end plate on wing bending moments, but these effects are believed to be small. The lateral center-of-pressure location obtained in the slotted tunnel was in fairly good agreement with 7 by 10 results, although slightly inboard above M = 0.90.

While some scatter of test points is evident in the basic data (figs. 6(d) and 8(d)) the over-all agreement is good up to M = 0.90. Above 0.90 Mach number the slotted-tunnel results indicated an inboard movement of the lateral center of pressure as the lift increased above $C_L \approx 0.30$, especially for the swept wing (fig. 8(d)). These results are consistent with the pitching-moment characteristics of the large swept wing (fig. 8(b)) and indicate a loss in lift over the outboard sections of the wing. Reasons for this behavior at high-subsonic Mach numbers are not apparent; however, reflected disturbances may produce marked changes in the flow and, therefore, may affect the characteristics at slightly supersonic Mach numbers.

Schlieren Photographs

Schlieren photographs of the flow over the small unswept wing in the $\frac{1}{8}$-open slotted tunnel at zero lift and at angles of attack of 10° and 20° are presented as figure 17. Schlieren photographs were made only for the small wing in order to observe the flow at high angles of attack which was not possible on the large wings due to strain-gage limitations at supersonic Mach numbers. The three-dimensional nature of the flow disturbances shown imposes difficulties in interpreting the schlieren photographs; however, interesting aspects of the flow phenomena may be seen. In all of these pictures, the direction of flow is from left to right, the location of the semispan model is defined by the shadow of the cutout in the front-surface mirror through which the wing was mounted. Irregularities at the edges of the cutout were caused by flaking of the mirror surface.

The stream area in which the flow is supersonic is defined roughly by the extent of the shock waves which in the zero-lift condition do not reach the tunnel walls at Mach numbers of 0.896 and 0.936. Above $M = 0.986$ the terminal shock moves rearward and the detached bow shock appears at $M = 1.037$. The intersection of the bow shock and the tunnel side wall creates the illusion of a second bow wave at Mach numbers between 1.050 and 1.154. At Mach numbers below 1.08 the shock waves are nearly normal to the stream and no reflected shocks would be expected since the flow along the wall downstream of the incident wave is subsonic. At higher Mach numbers the presence of reflected shocks, first appearing as Mach reflections of the incident wave, indicate that the slot area was insufficient to permit the air directed toward the wall to leave the test section at the pressure difference across the incident wave. Above a Mach number of 1.2 the reflection of the incident bow shock reaches the plane of the model at a point well behind the trailing edge; the jet boundary would therefore be expected to have no influence on the model characteristics.

Although the shock patterns at angles of attack of 10° and 20° differ markedly from those of zero lift, the reflection phenomena are the same. Clear-cut reflections of the bow shock at $M = 1.26$ and 1.30 appear to pass behind the model. The absence of reflected shock waves in the schlieren photographs cannot, of course, be interpreted as indicating that the flow over the model is not influenced by the tunnel boundary at supersonic speeds below which reflected shocks occur. However, it appears from these photographs as well as from the force data presented that the disturbances reflected from this $\frac{1}{8}$- open slotted wall below $M = 1.154$ are of small intensity and that their influence on the model is not great.

CONCLUSIONS

The present investigation was one of an exploratory nature to
provide an indication of tunnel-wall effects that might be encountered
when testing lifting wings in a slotted-throat wind tunnel at transonic
Mach numbers. These limited results do not permit a generalized evalua-
tion of effects to be expected in slotted tunnels of arbitrary geometry
but point out some important considerations incident to transonic testing
in a slotted tunnel.

The results of this investigation indicated the following conclusions:

1. Tunnel choking was eliminated and accompanying blockage effects
were alleviated by the slotted test section throughout the lift and Mach
number range investigated for all the wings tested.

2. In general, the transonic aerodynamic characteristics of the
four lifting wings tested in the $\frac{1}{8}$ - open slotted tunnel were consistent
with 7- by 10-foot tunnel results throughout the Mach number range
investigated.

3. The amount of open area appreciably affected the lift-curve
slopes for all the wings at subsonic Mach numbers; an increase in open-
area ratio resulting in a decrease in lift-curve slope.

4. Lift-curve slopes for the unswept wings at supersonic speeds
were affected predominantly by relative model size. In general, the
increase in jet-boundary interference effects in the slotted tunnel,
associated with an increase in model size, was more pronounced for the
swept wings than for the unswept wings.

5. Schlieren photographs indicate that the slotted boundaries used
in this investigation did not eliminate reflection of shock waves.

Langley Aeronautical Laboratory
        National Advisory Committee for Aeronautics
                Langley Field, Va.

REFERENCES

1. Goodman, Theodore R.: Wall Interference on Lifting Wings in Wind Tunnels with Transonic Throat Configurations. Rep. No. AD-594-A-1, Cornell Aero. Lab., Inc., Oct. 1949.

2. Wright, Ray H., and Ward, Vernon G.: NACA Transonic Wind-Tunnel Test Sections. NACA RM L8J06, 1948.

3. Donlan, Charles J., Myers, Boyd C., II, and Mattson, Axel T.: A Comparison of the Aerodynamic Characteristics at Transonic Speeds of Four Wing-Fuselage Configurations as Determined from Different Test Techniques. NACA RM L50H02, 1950.

4. Kemp, William B., Jr., Goodson, Kenneth W., and Booth, Robert A.: Aerodynamic Characteristics at a Mach Number of 1.38 of Four Wings of Aspect Ratio 4 Having Quarter-Chord Sweep Angles of 0°, 35°, 45°, and 60°. NACA RM L50G14, 1950.

(a)   Model installation in slotted tunnel.

End plate used in slotted-tunnel tests.

.032 thick

.013 thick

End plate used in all tests.

.032 thick

End plates used in 7 by 10 tests.

All dimensions in inches.

Reference axis, $\bar{c}/4$

45°

0°

Scale, inches
0   1   2   3   4   5
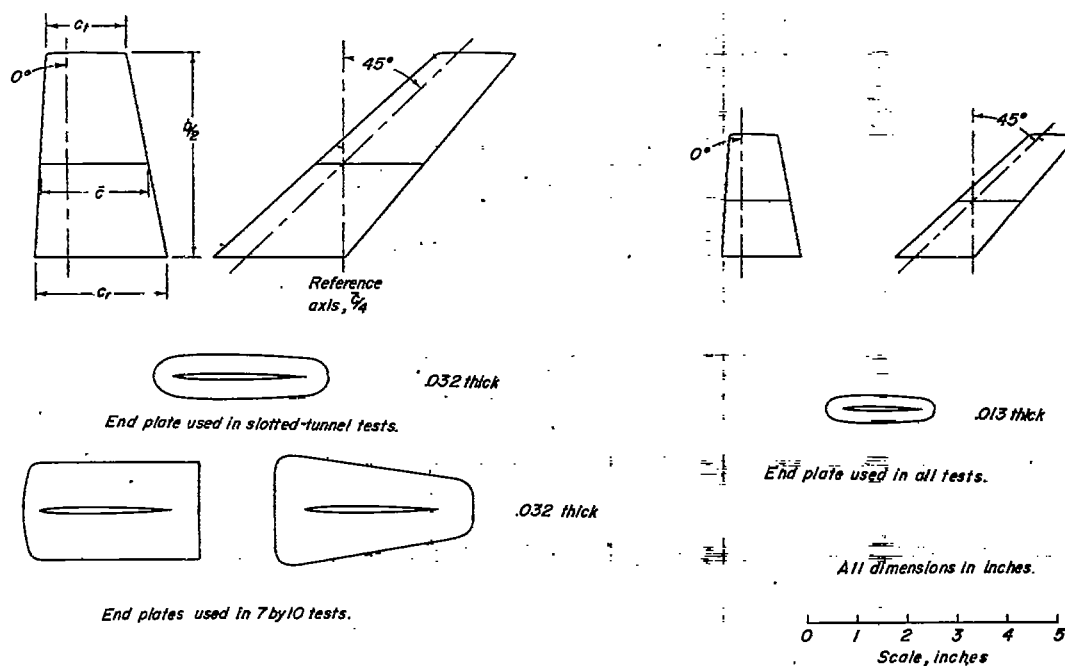
Tabulated Geometric Characteristics

Large wings

Aspect ratio	4.0
Taper ratio	0.6
Airfoil section parallel to free stream	NACA 65A006

Small wings

Wing area, S	0.125 sq ft
Wing span, b	8.484 in.
Mean aerodynamic chord, $\bar{c}$	2.166 in.
Root chord, c_r	2.652 in.
Tip chord, c_t	1.591 in.

Wing area, S	0.045 sq ft
Wing span, b	5.092 in.
Mean aerodynamic chord, $\bar{c}$	1.300 in.
Root chord, c_r	1.591 in.
Tip chord, c_t	0.955 in.

NACA

(b)   Model configuration.

Figure 1.- Drawing of models used in tests in the slotted tunnel and in
the Langley high-speed 7- by 10-foot tunnel reflection plane, showing
the model installation in the slotted tunnel.
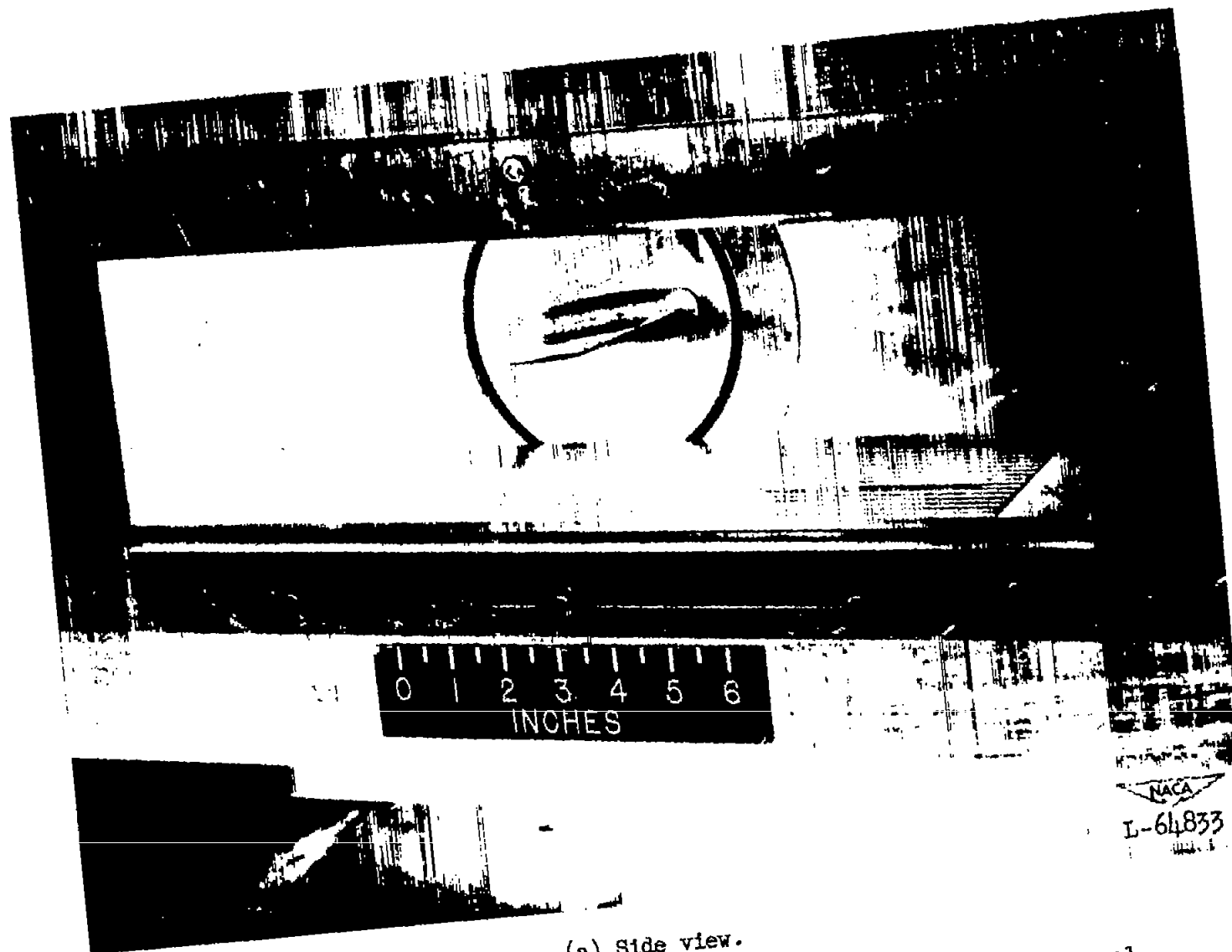
(a) Side view.

Figure 2.- Photograph of large unswept wing mounted in the slotted tunnel.

L-64833

17

L-64834
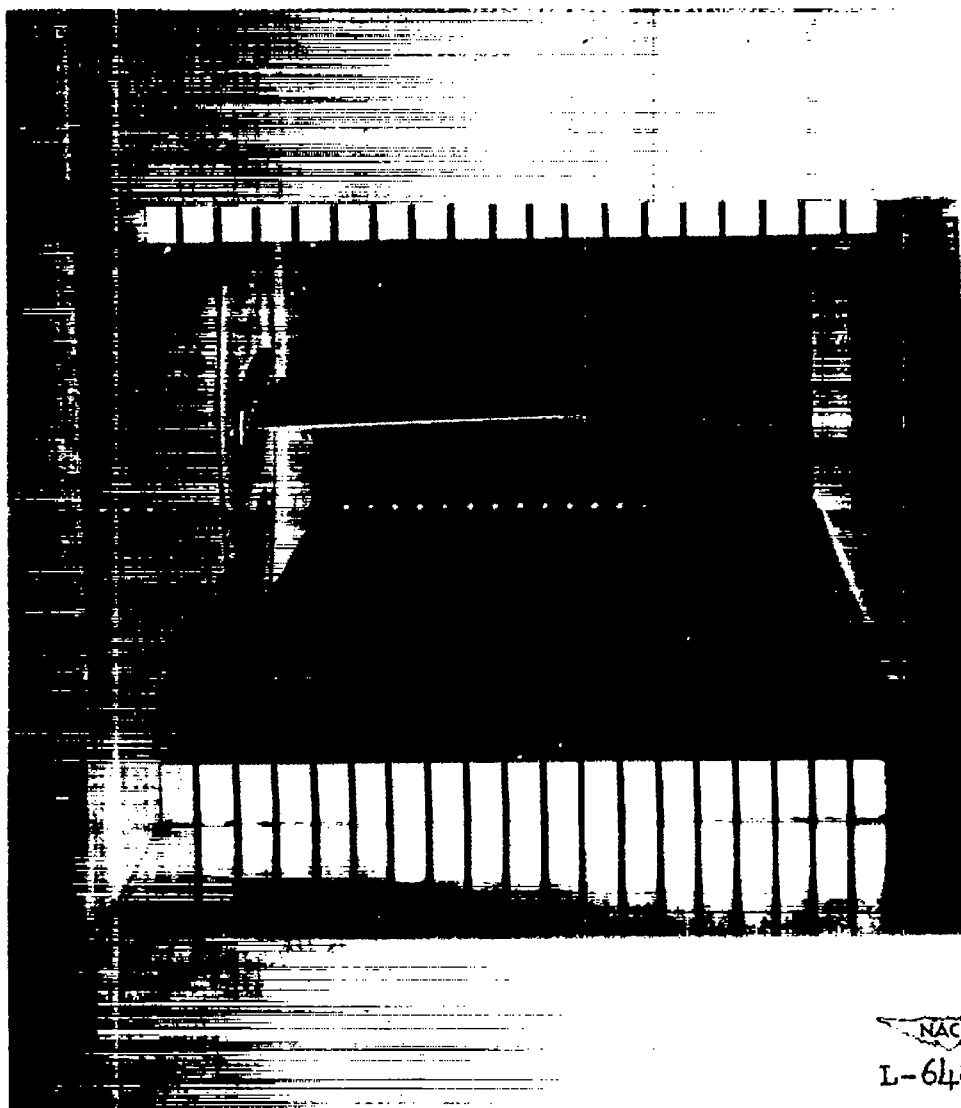
(b) Rear view.

Figure 2.- Concluded.
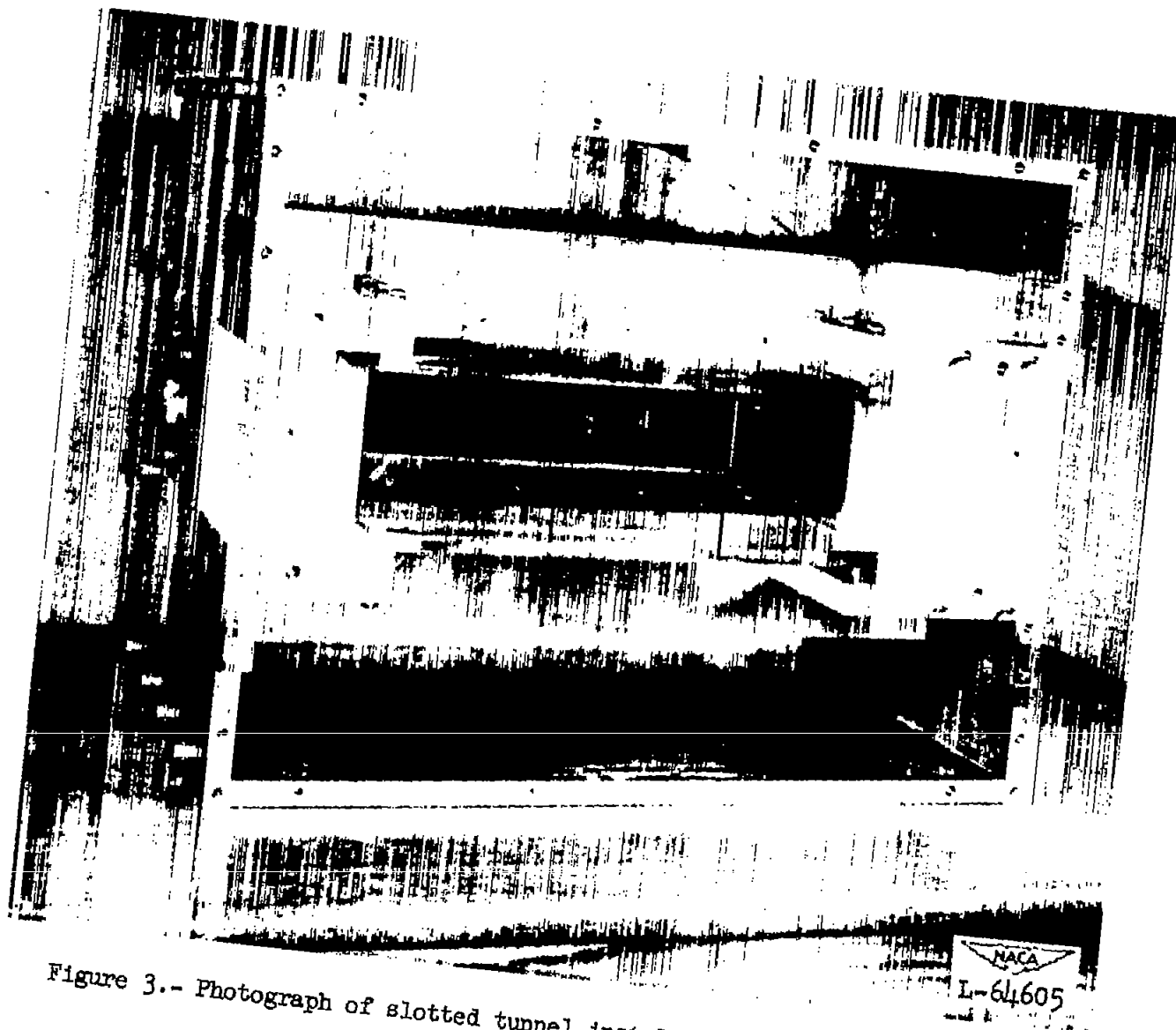
Figure 3.- Photograph of slotted tunnel installed in the pressure chamber with one side removed.

L-64605
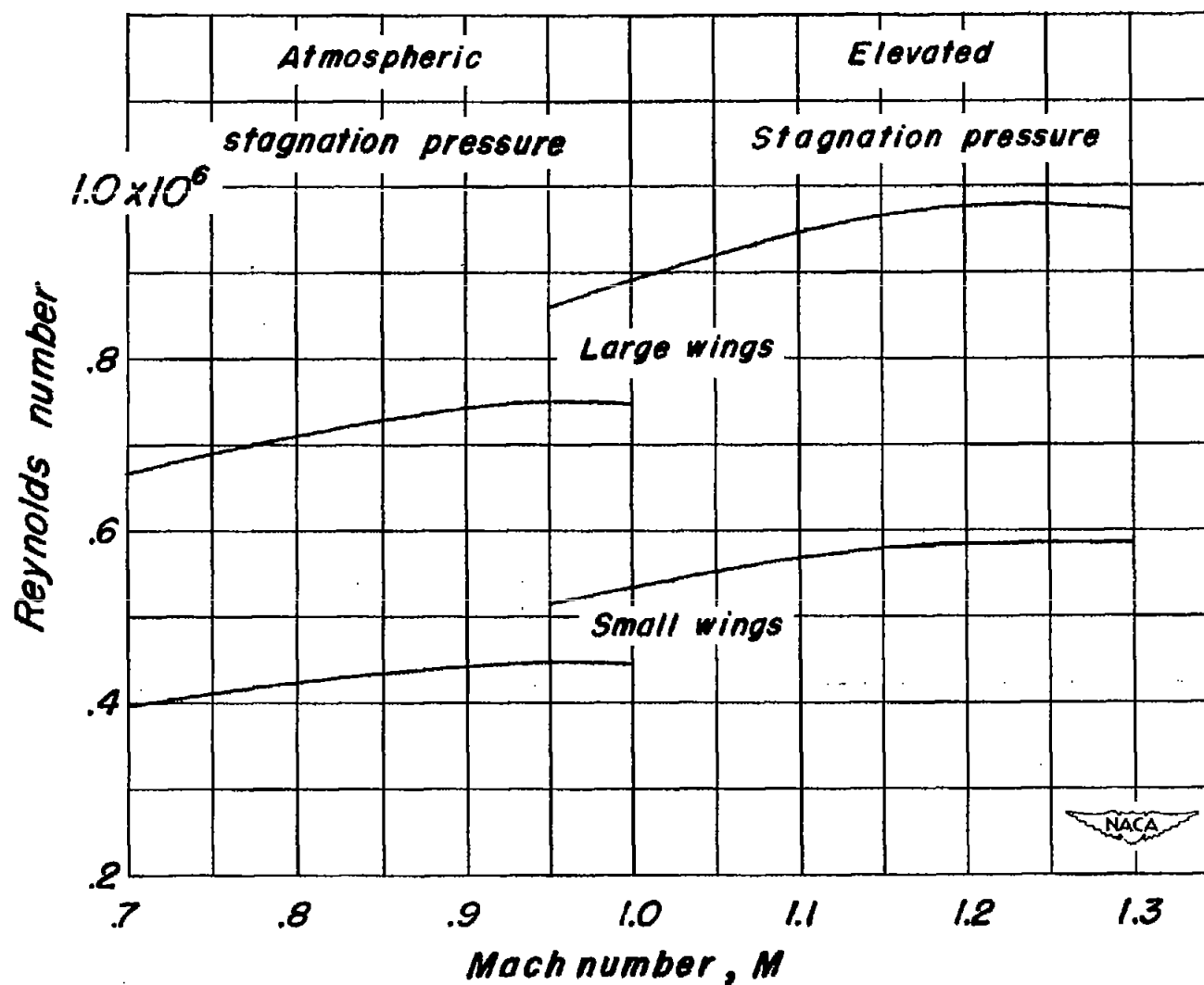
Figure 4.- Variation of Reynolds number with Mach number for the tests in the slotted tunnel.
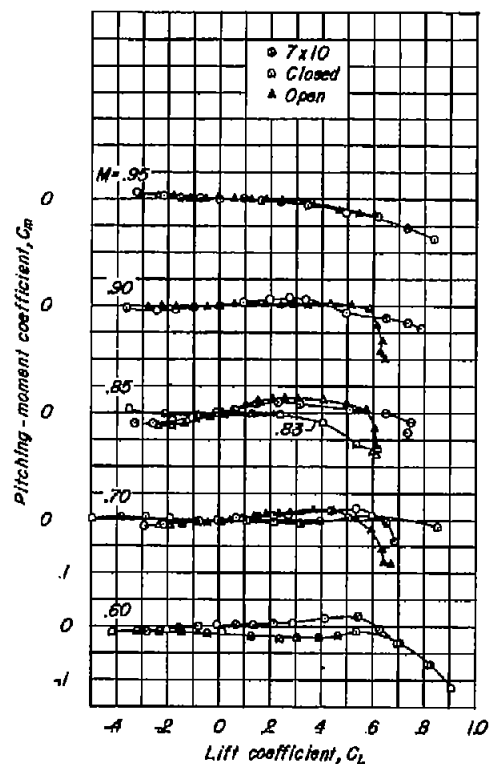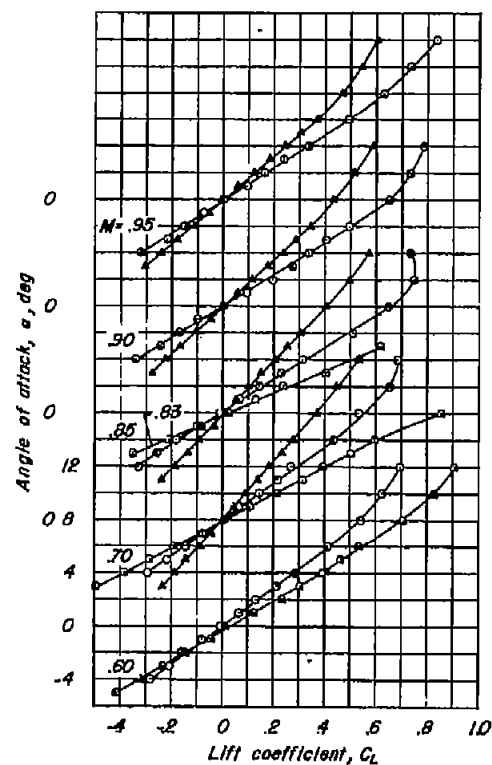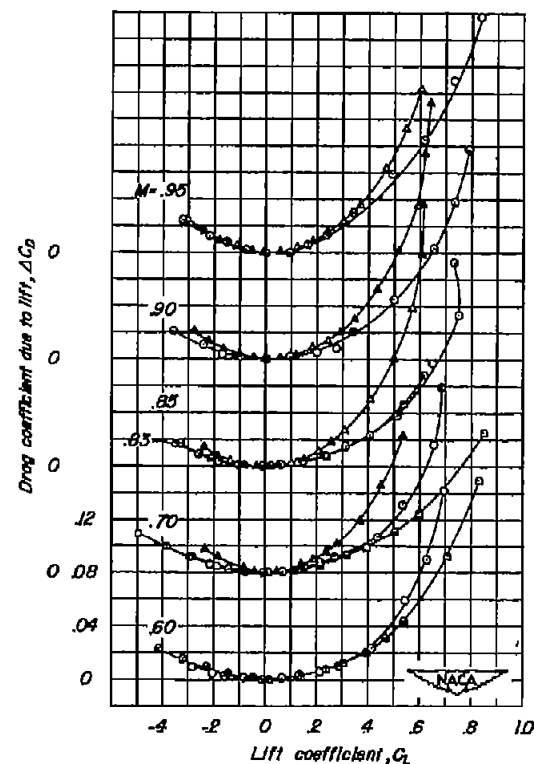
A=0° Large wing

Figure 5.- Comparison of aerodynamic characteristics of the large unswept
wing tested in the Langley high-speed 7- by 10-foot tunnel and in the
small tunnel with open and closed horizontal boundaries.
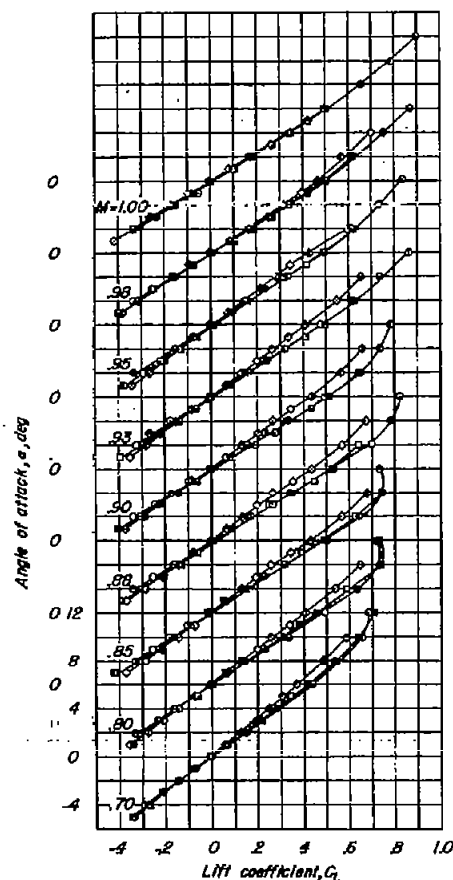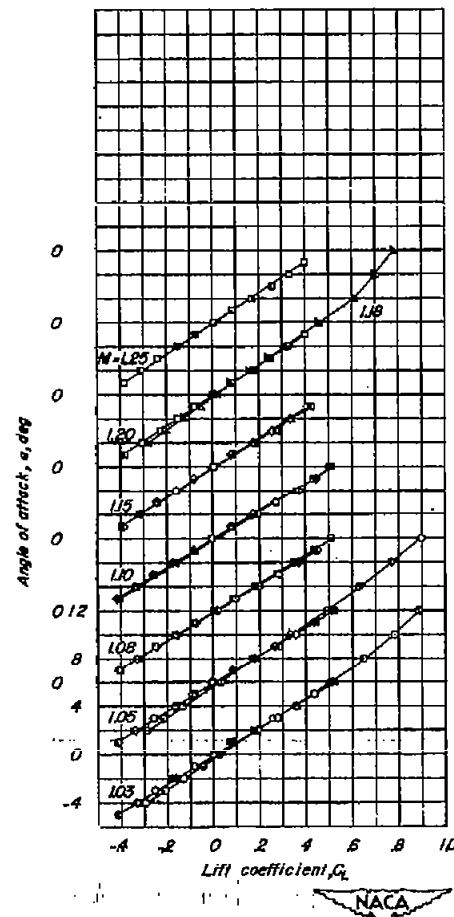
(a) α against C_L.

Figure 6.- Comparison of aerodynamic characteristics of the large unswept wing tested in the slotted tunnel and the Langley high-speed 7- by 10-foot tunnel.
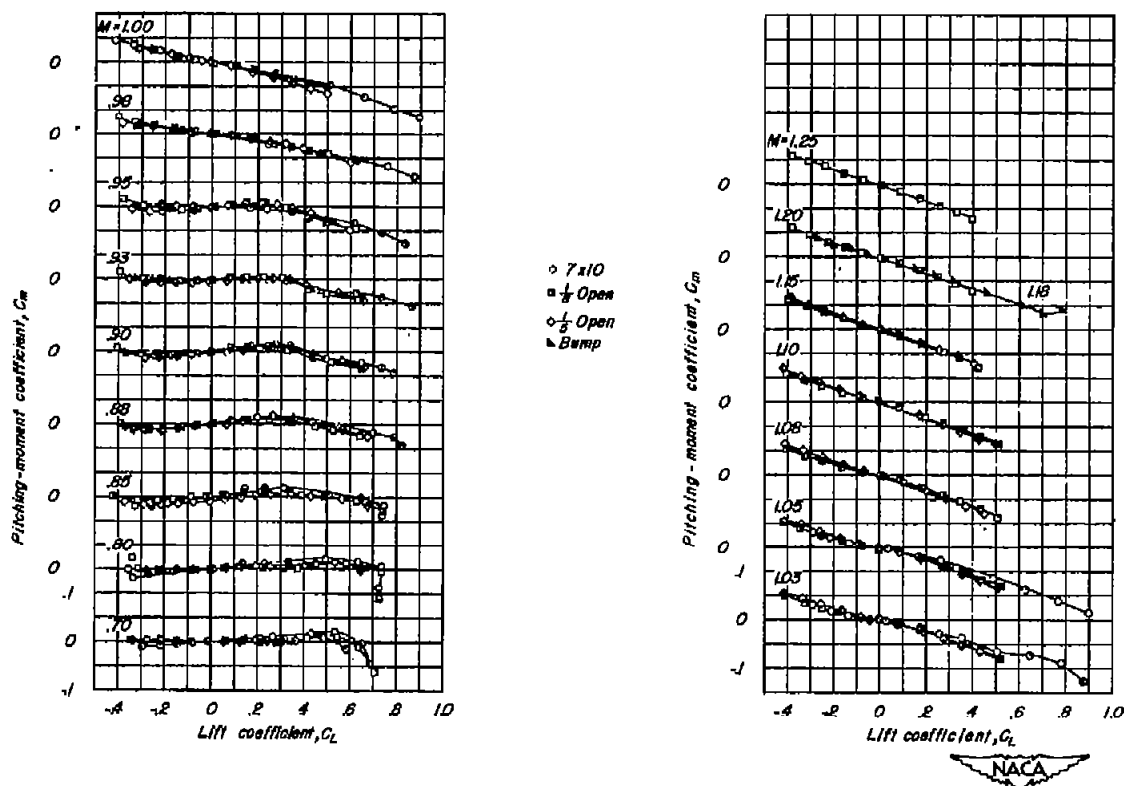
A=0° Large wing

(b) C_m against C_L.

Figure 6.- Continued.
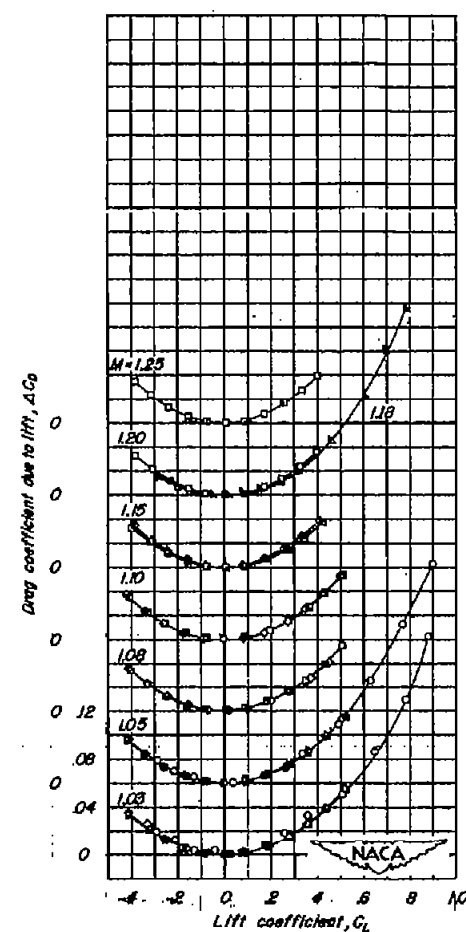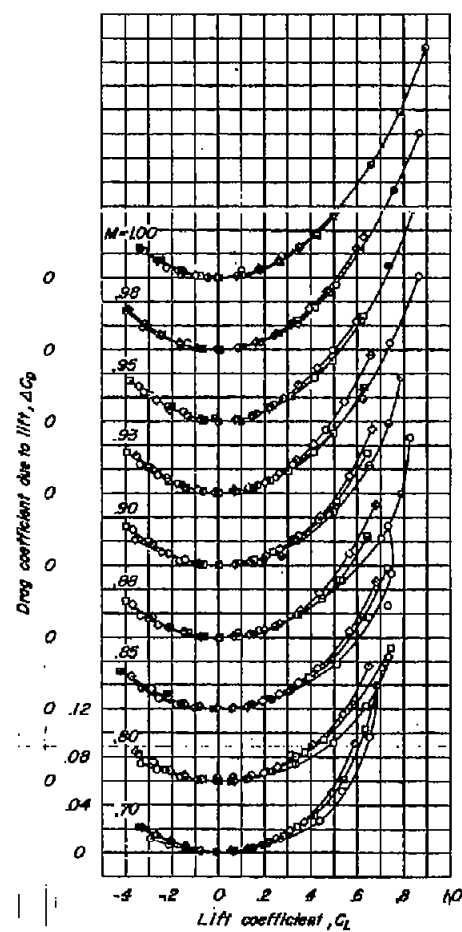
(c) ΔC_D against C_L.

Figure 6.- Continued.
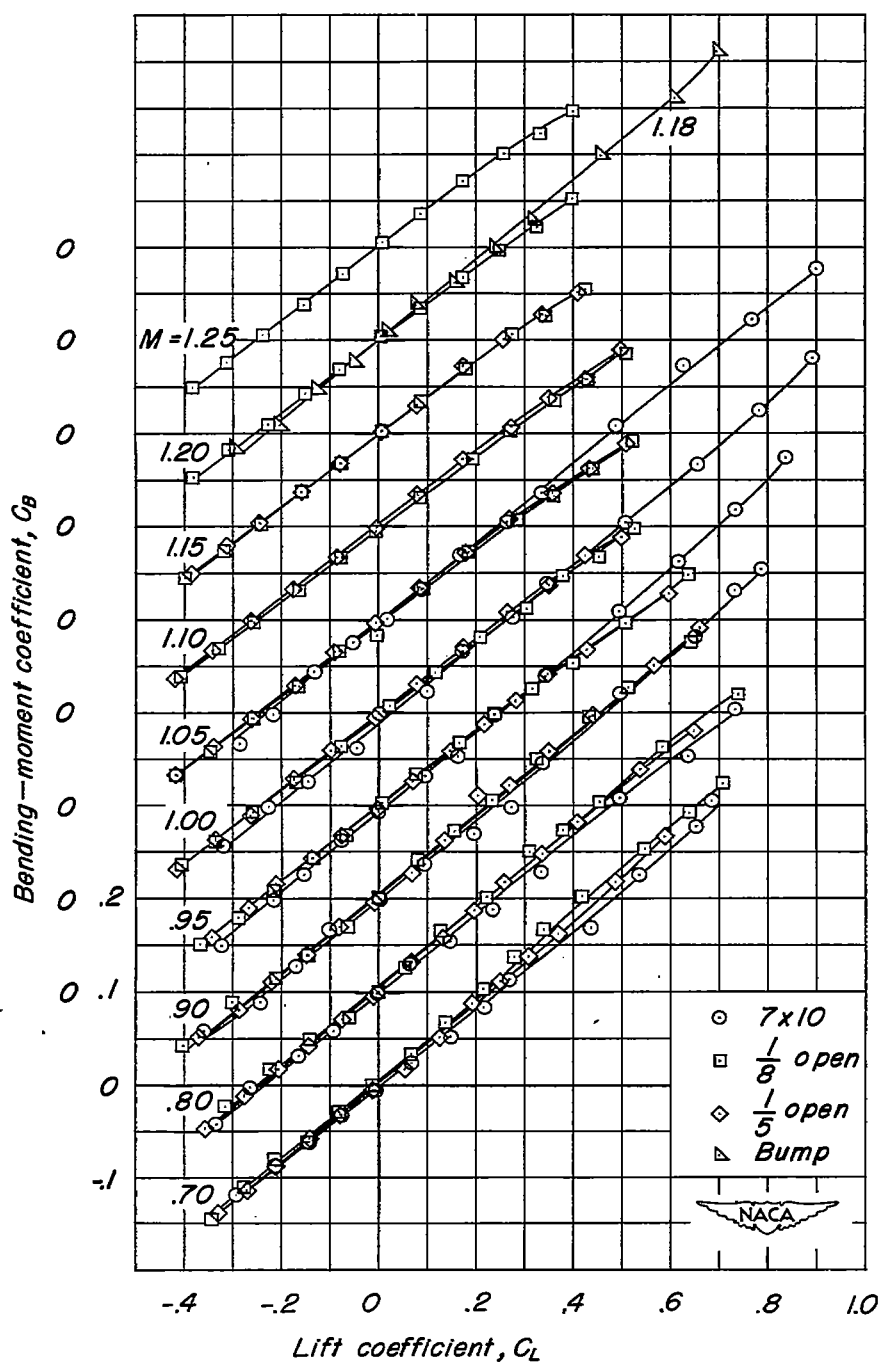
$\Lambda = 0°$ Large wing

(d) C_B against C_L.

Figure 6.- Concluded.
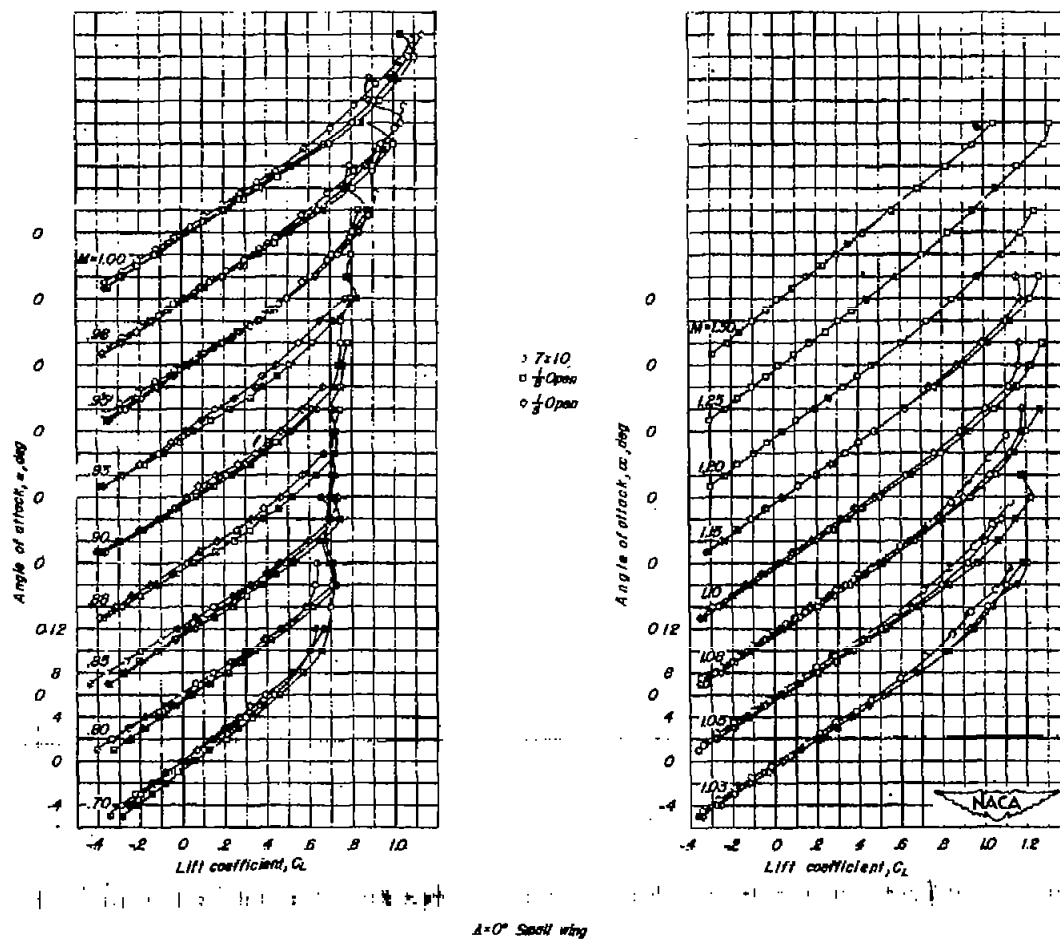
(a) α against C_L.

Figure 7.- Comparison of aerodynamic characteristics of the small unswept wing tested in the slotted tunnel and the Langley high-speed 7- by 10-foot tunnel.
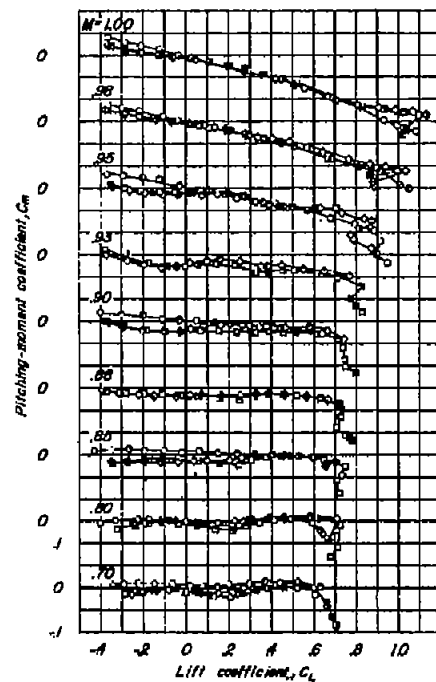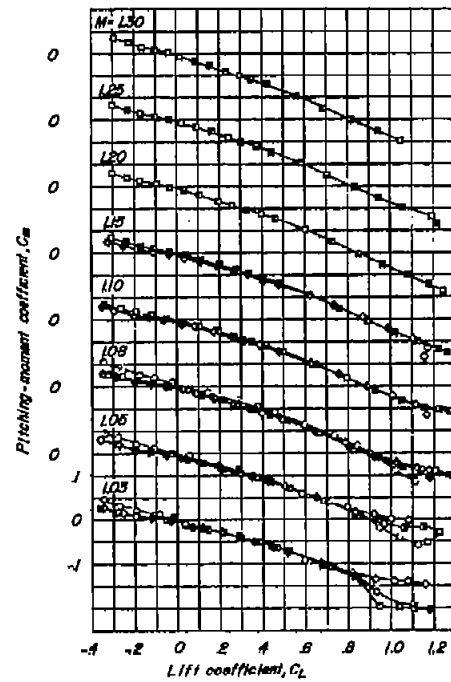
(b) C_m against C_L.

Figure 7.- Continued.
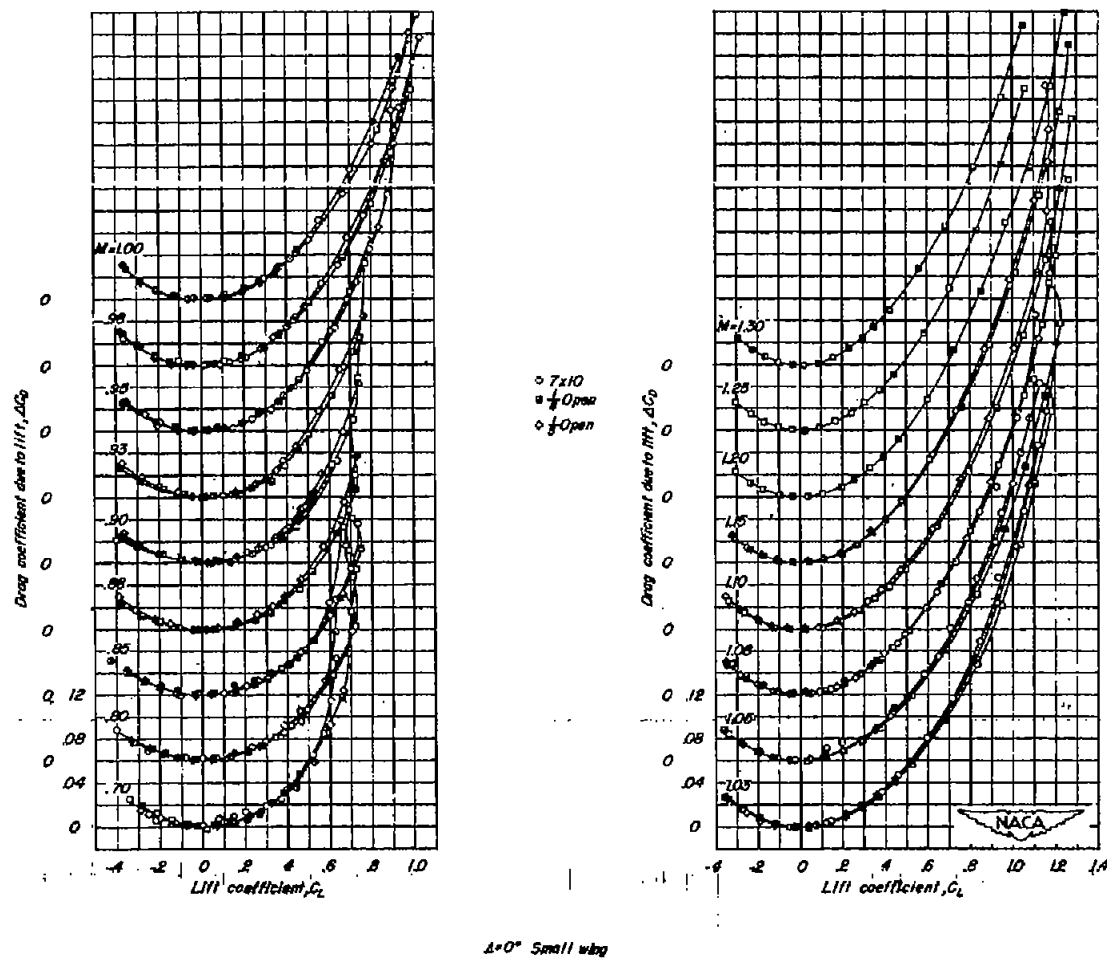
(c) ΔC_D against C_L.

Figure 7.- Concluded.
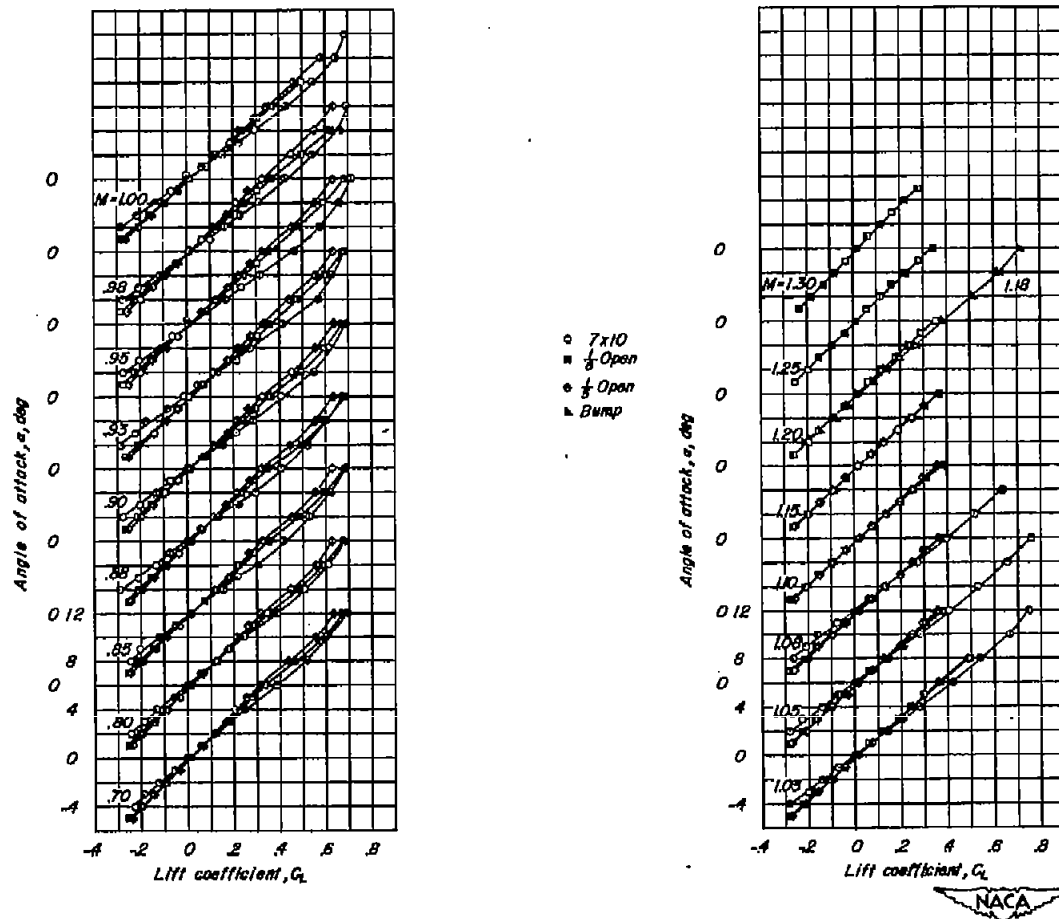
(a) α against C_L.

Figure 8.- Comparison of aerodynamic characteristics of the large 45° swept-
back wing tested in the slotted tunnel and the Langley high-speed 7- by
10-foot tunnel.

(b) C_m against C_L.

Figure 8.- Continued.

(c) ΔC_D against C_L .
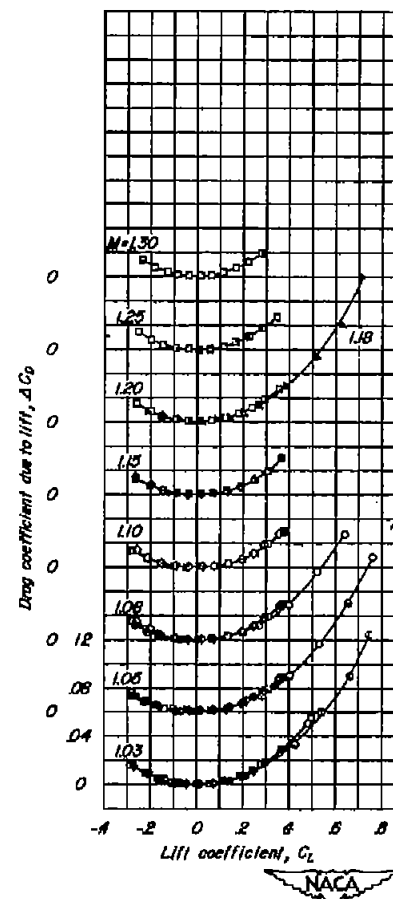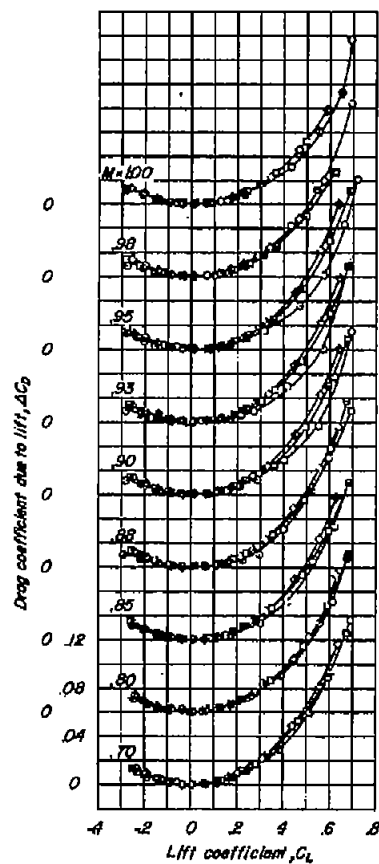
Figure 8.—, Continued.
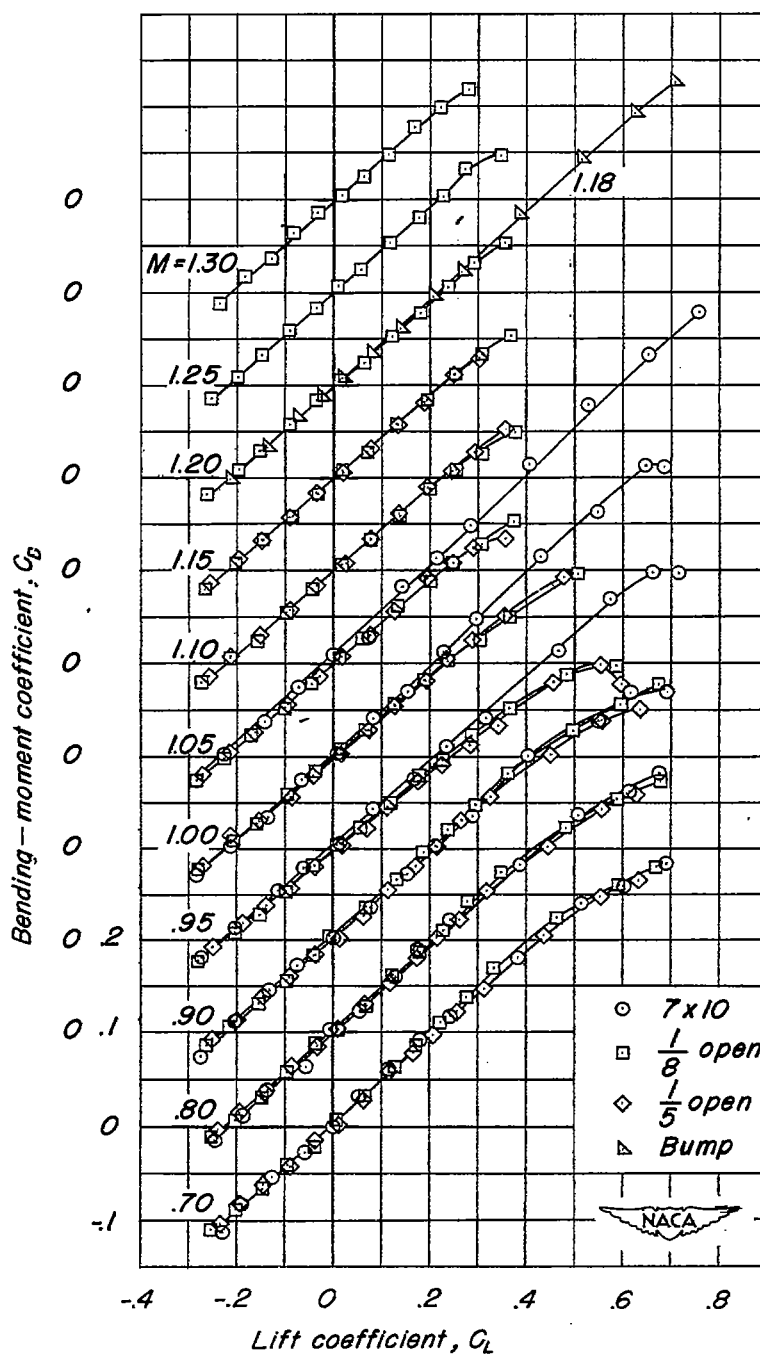
$\Lambda = 45°$ Large wing

(d) C_B against C_L.

Figure 8.- Concluded.
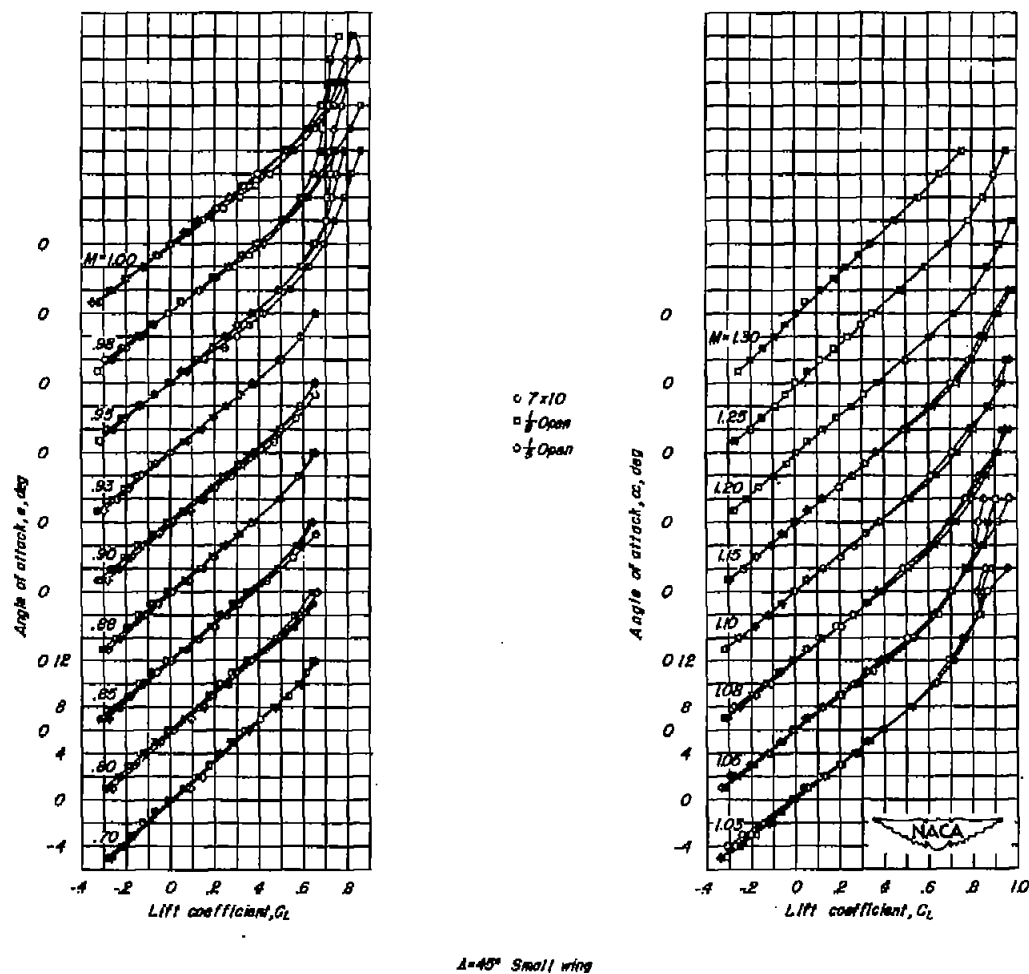
(a) α against C_L.

Figure 9.- Comparison of aerodynamic characteristics of the small 45° swept-
back wing tested in the slotted tunnel and the Langley high-speed 7- by
10-foot tunnel.
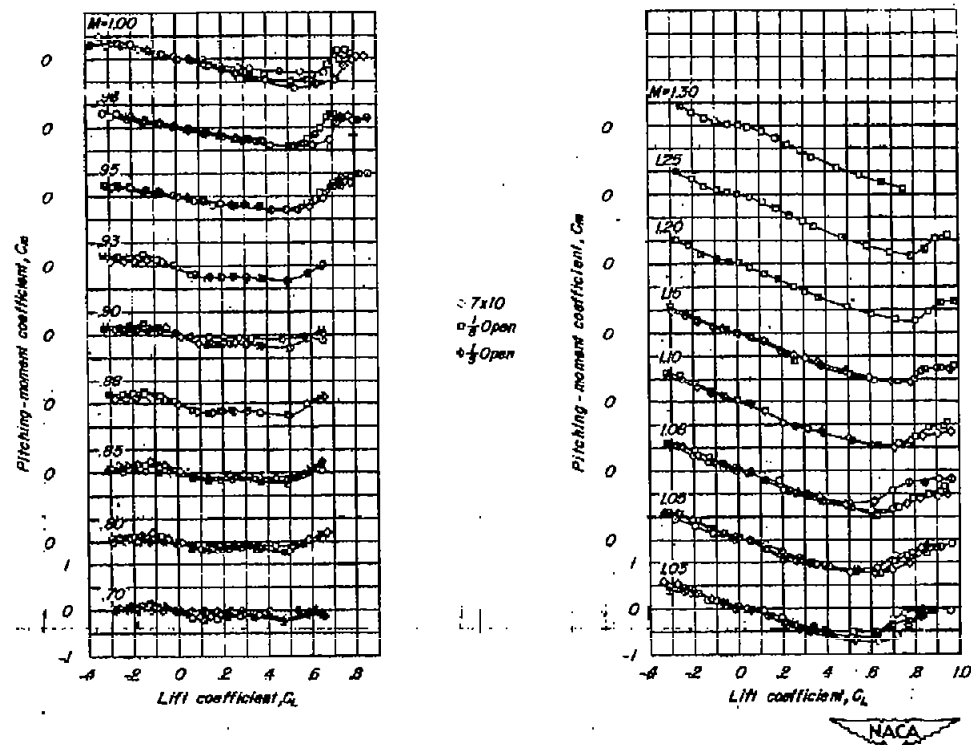
(b) C_m against C_L.

Figure 9.- Continued.
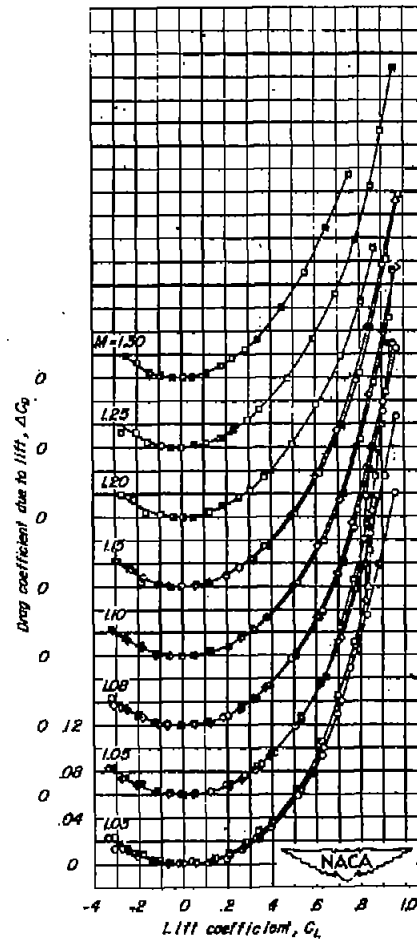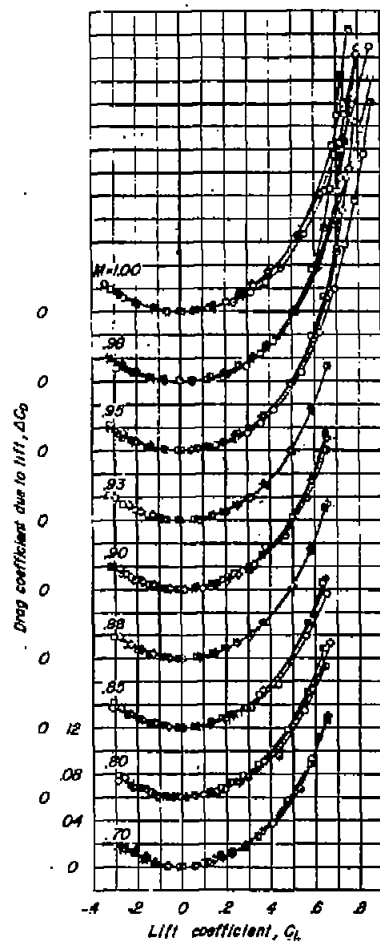
$A=45°$ Small wing

(c) ΔC_D against C_L.

Figure 9.- Concluded.
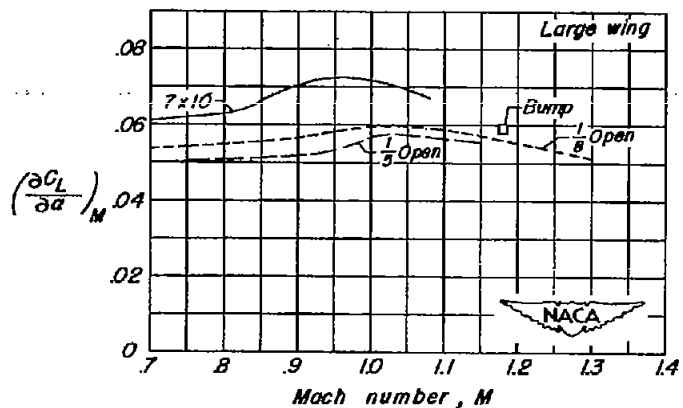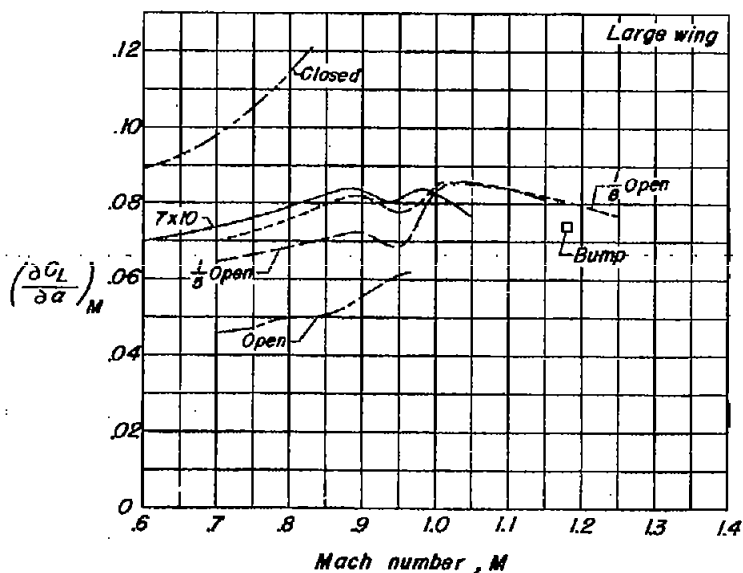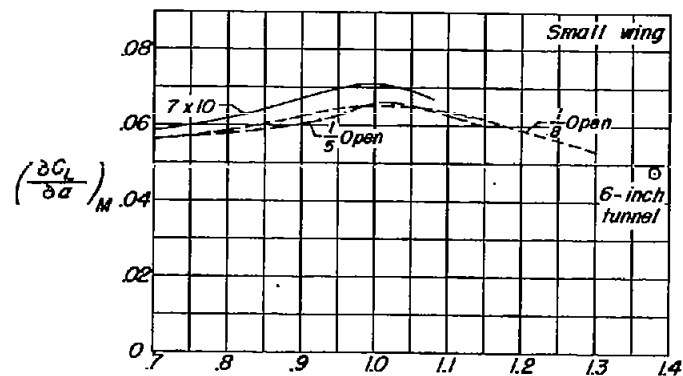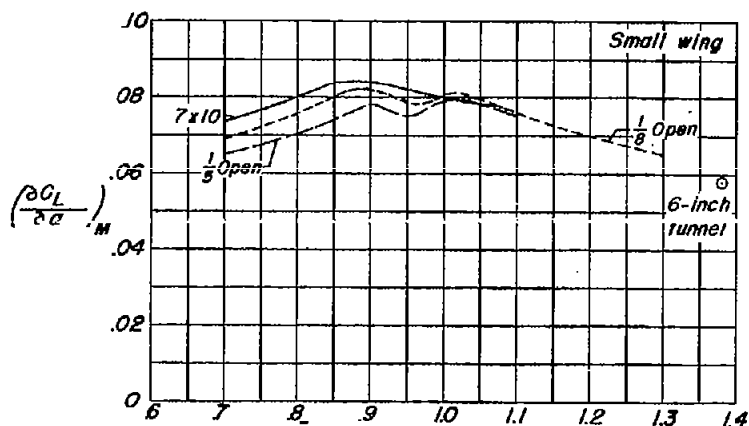
Figure 10.- Summary of lift characteristics obtained in the slotted tunnel
and the Langley high-speed 7- by 10-foot tunnel.
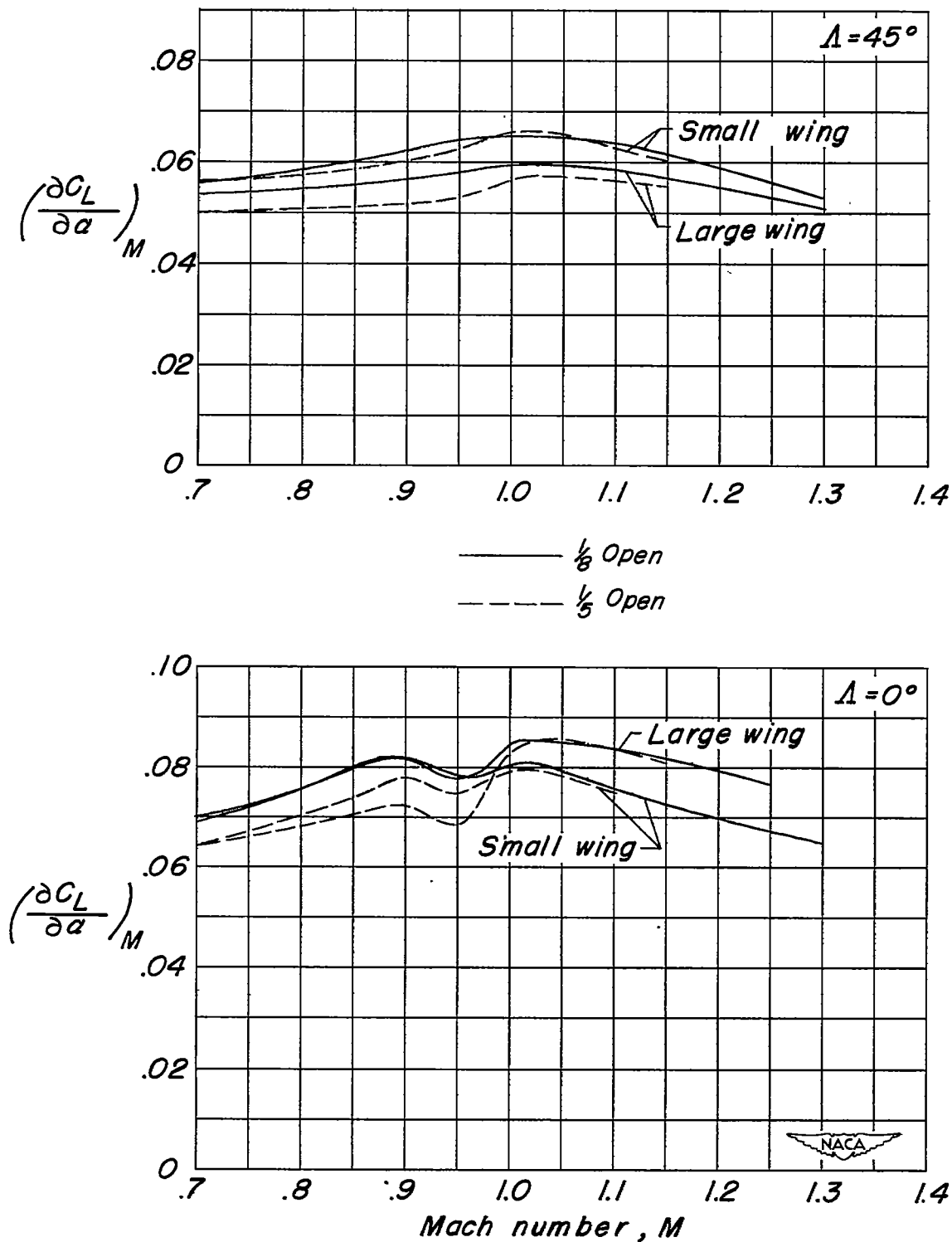
Figure 11.- Effect of model size and slot area on lift characteristics in the slotted tunnel.
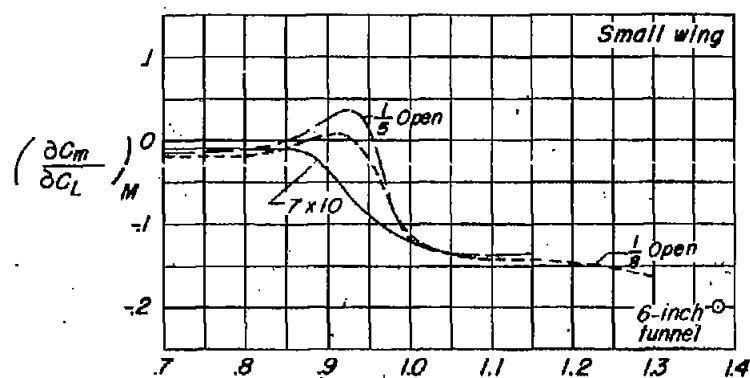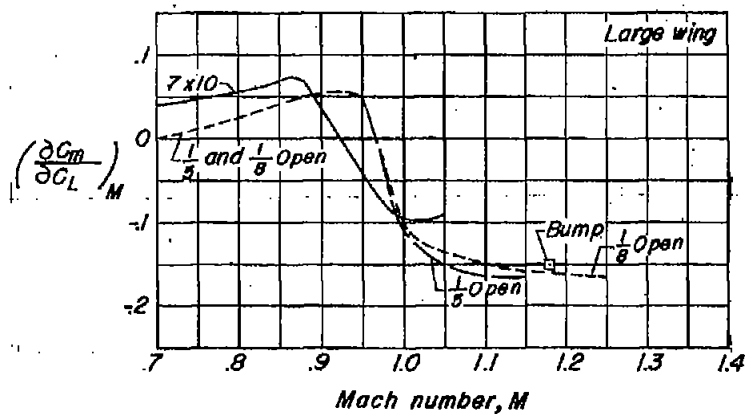
Figure 12.- Summary of pitching-moment characteristics obtained in the
slotted tunnel and the Langley high-speed 7- by 10-foot tunnel.
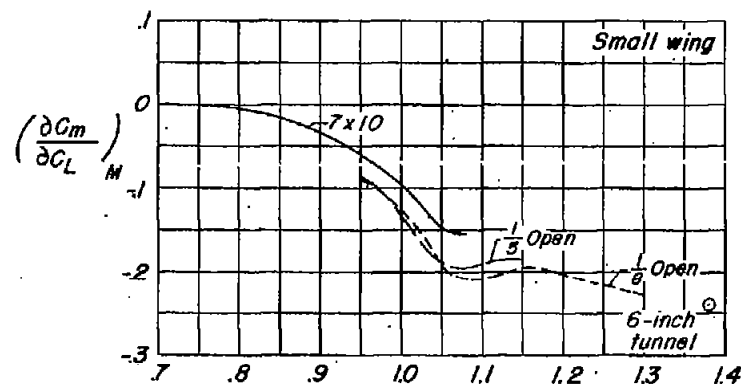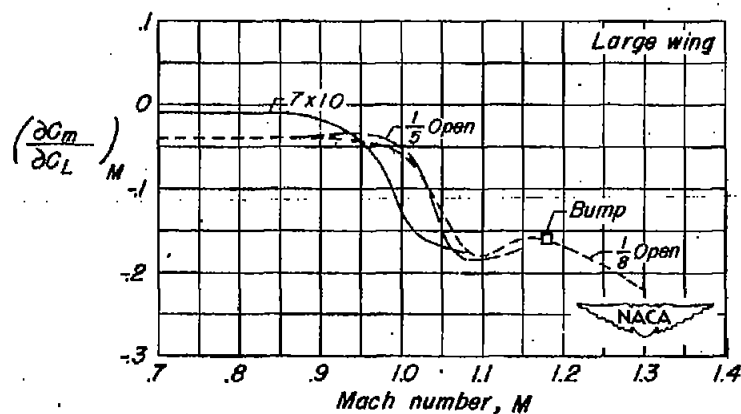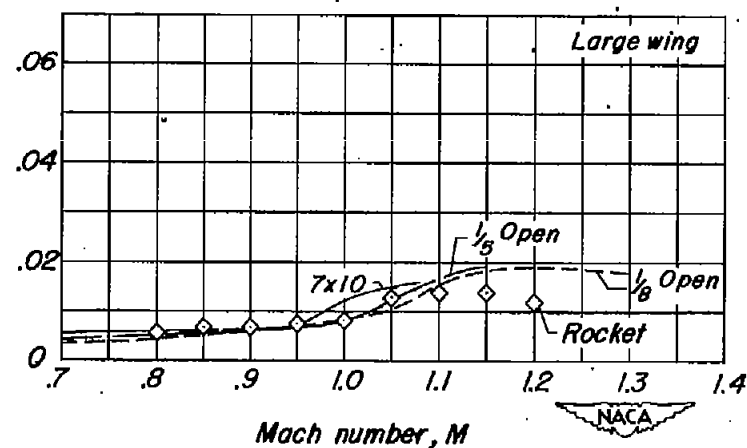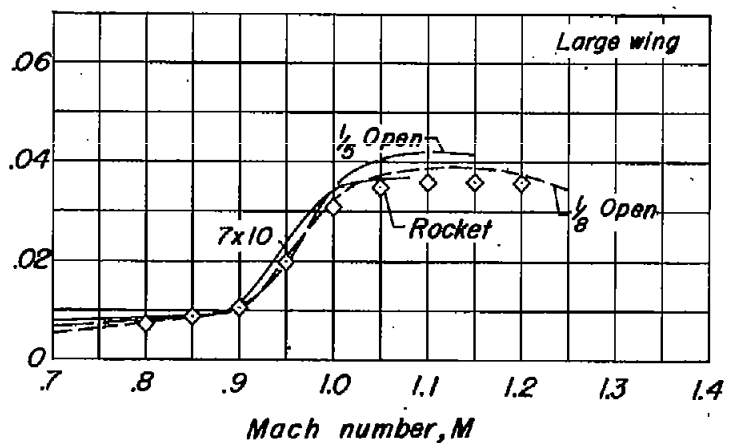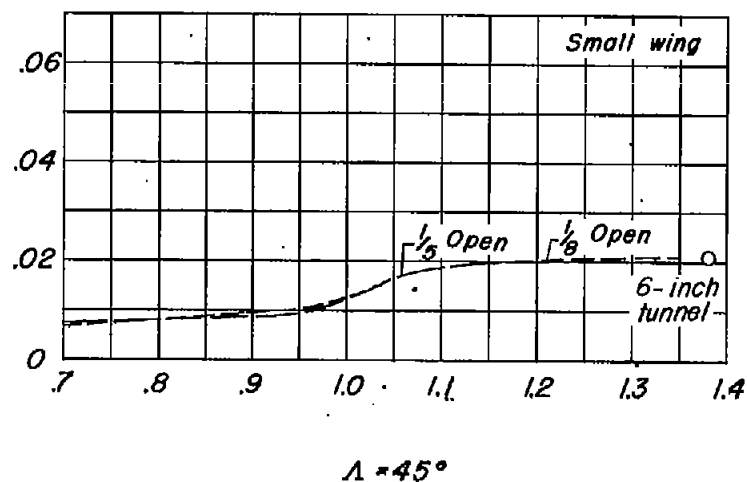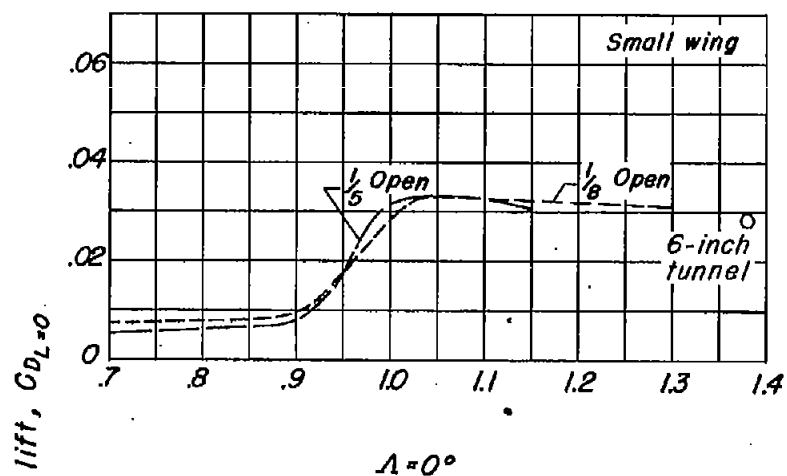
Figure 13.- Summary of minimum-drag characteristics obtained in the slotted
tunnel and the Langley high-speed 7- by 10-foot tunnel.
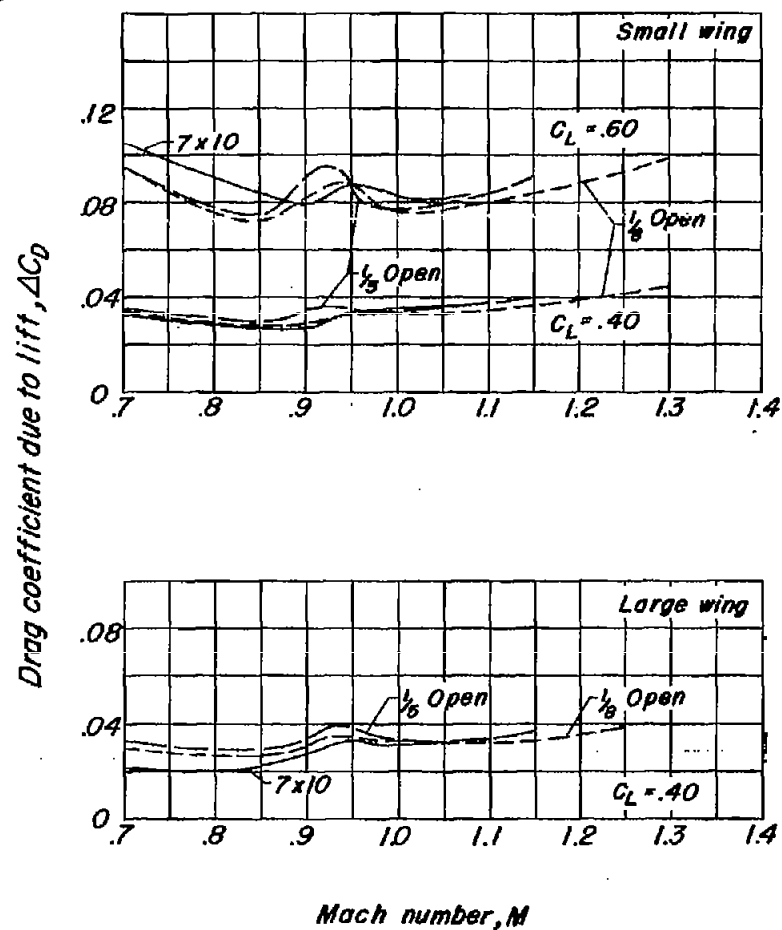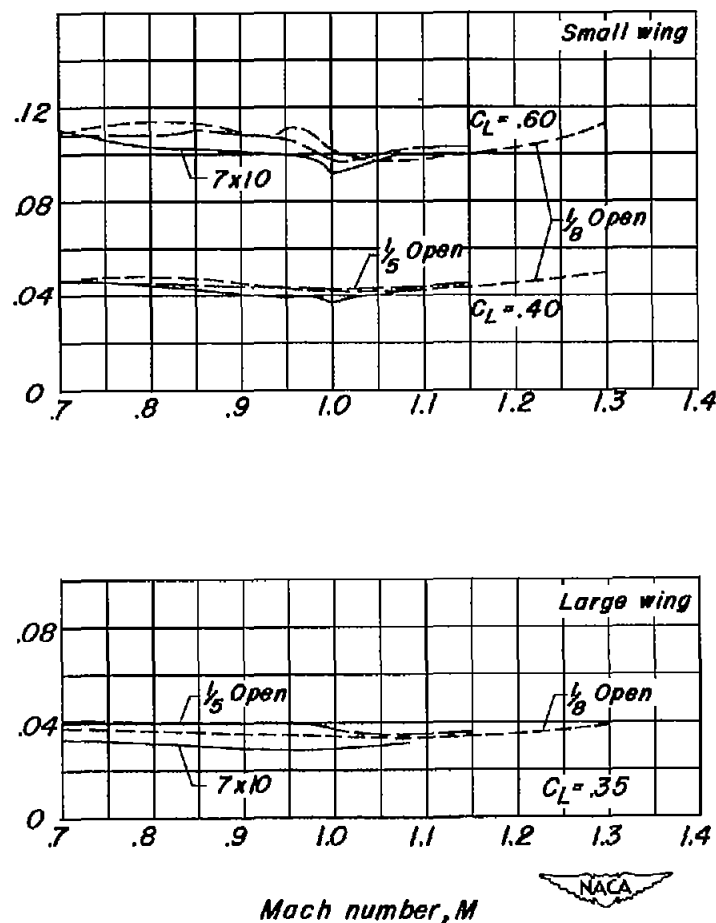
(a) Drag coefficient due to lift.
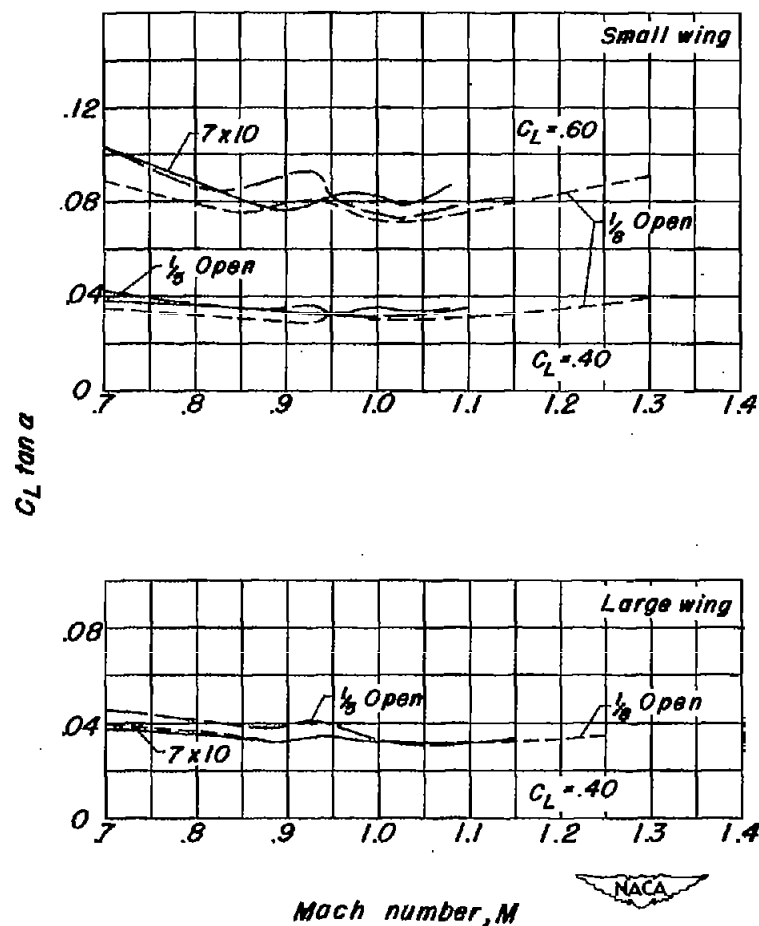
(b) $C_L \tan \alpha$.

Figure 14.- Summary of drag due to lift for the unswept wings tested in the slotted tunnel and the Langley high-speed 7- by 10-foot tunnel.

(a) Drag coefficient due to lift.

(b) C_L tan α.

Figure 15.- Summary of drag due to lift for the 45° sweptback wings tested in the slotted tunnel and the Langley high-speed 7- by 10-foot tunnel.
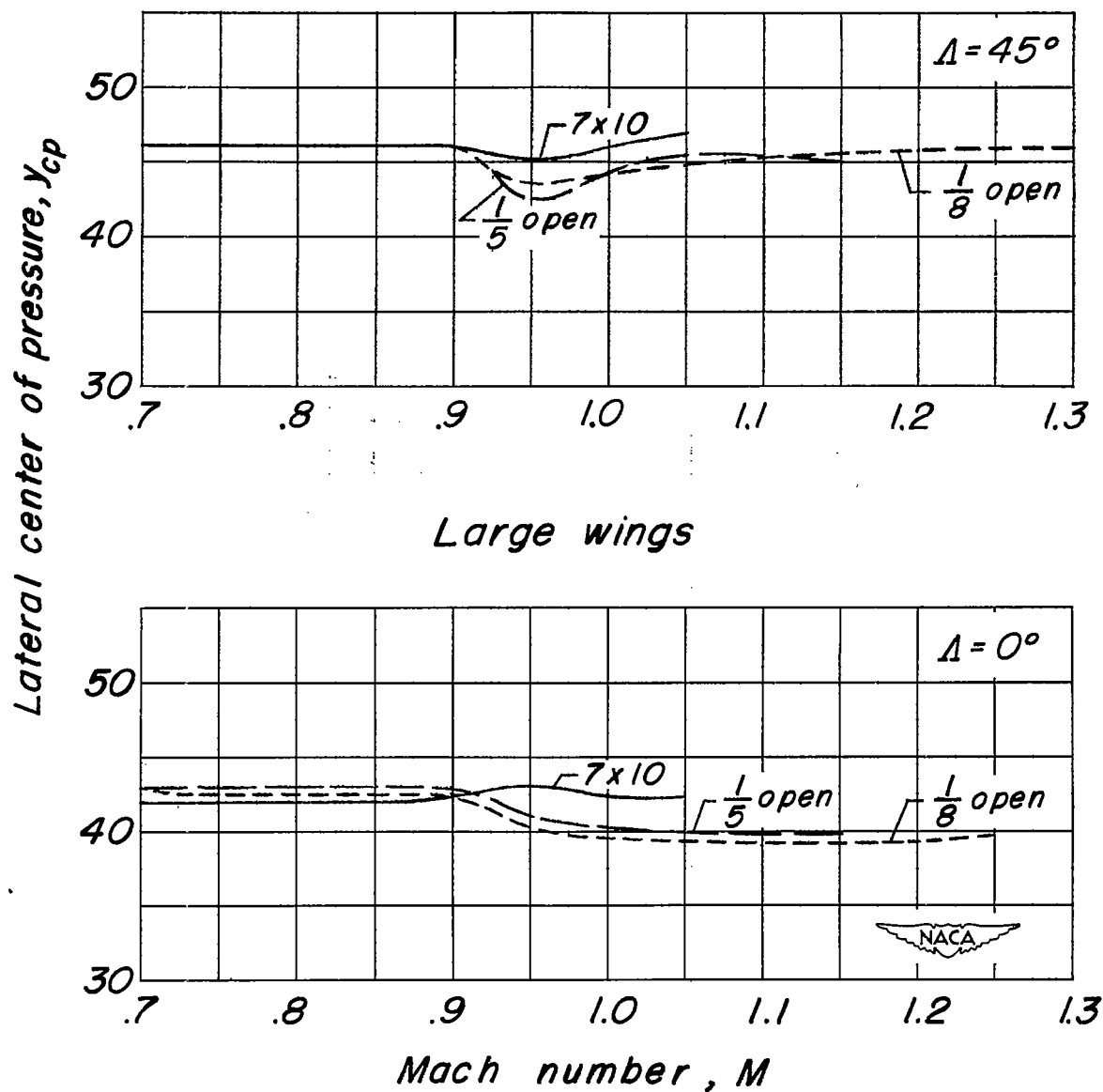
Figure 16.- Lateral center-of-pressure location for the large wings tested in the slotted tunnel and the Langley high-speed 7- by 10-foot tunnel.
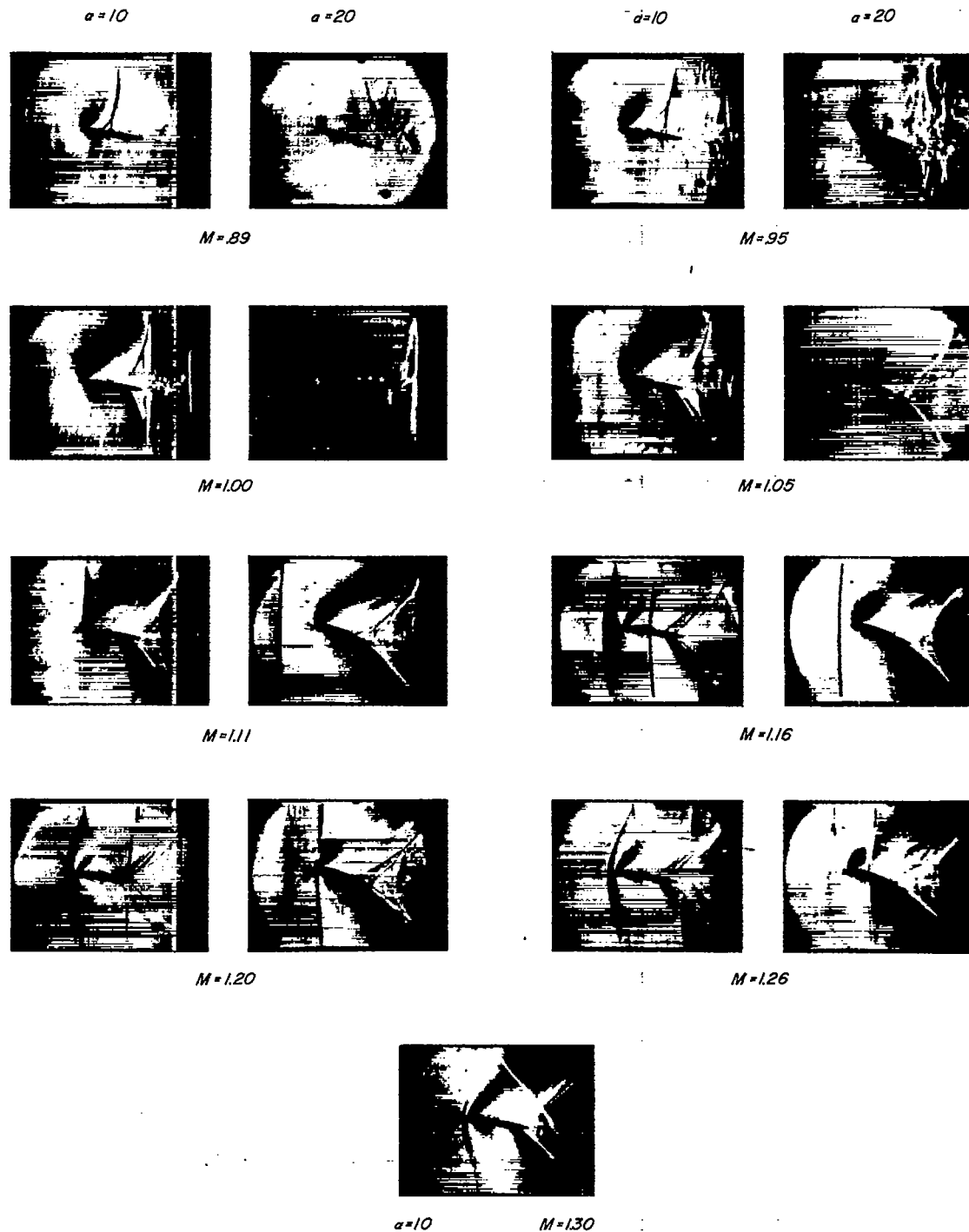
(a)   α = 0°.

L-70776

Figure 17.- Schlieren photographs of the flow about the small unswept wing in the $\frac{1}{8}$-open slotted tunnel.

$a = 10$ $a = 20$ $a = 10$ $a = 20$

M = .89   M = .95

M = 1.00   M = 1.05

M = 1.11   M = 1.16

M = 1.20   M = 1.26

$a = 10$ M = 1.30

(b)   α = 10° and 20°.

Figure 17.- Concluded.

L-70777